AQUARIUS/SAC-D

Aquarius Salinity Validation Analysis

Aquarius Project Document: **AQ-014-PS-0016**
28 February 2018

Data Version 5.0

Aquarius Salinity Validation Analysis

PREPARED BY (CUSTODIAN):

__HSUN-YING KAO___ _____
Name Date

APPROVED BY:

_GARY LAGERLOEF_____ _____
Name Date

_____ _____
Name Date

_____ _____
Name Date

DOCUMENT CHANGE LOG

Change Number	Change Date	Pages Affected	Changes/ Notes	General Comments
-	10 November 2017	All	1st Draft	
	1 December 2017	All	2nd Draft	
	5 December 2017	All	3rd Draft	
	28 February 2018 Revision 1	17-18, 20-22, 39-40	Revision 1: Add Triple point analysis, correct Table 2, augment Summary	G.Lagerloef and H.Kao, with review comments from L.Hong, T.Meissner, T.Lee, J. Vazquez, P.Hacker

Aquarius Salinity Validation Analysis; Data Version 5.0

Lead Author: Hsun-Ying Kao (Earth & Space Research)
Contributing Authors: Gary Lagerloef (Earth & Space Research, Aquarius Principal Investigator), Tony Lee (Jet Propulsion Lab), Oleg Melnichenko (University of Hawaii), Peter Hacker (University of Hawaii)

Document Reviewers: David LeVine (NASA Goddard Space Flight Center), Tony Lee (Jet Propulsion Lab), Liang Hong (Science Application Intl. Corp.), Jorge Vazquez (Jet Propulsion Lab), Peter Hacker (University of Hawaii), Gary Lagerloef (Earth & Space Research, Aquarius Principal Investigator)

Table of Contents

1. Introduction

The purpose of this report is to document the Aquarius sea surface salinity (SSS) measurement uncertainty characteristics, including residual errors in the final version (**V5.0**) of the Aquarius data, which was released 7 December 2017. We document the progressive improvement from V2.0 to V5.0 by comparing each version of Aquarius data with *in situ* data. It should be noted that the matchup statistics (e.g., Section 2, 5 and 6) between Aquarius and *in situ* observations not only include Aquarius SSS uncertainty, but also the sampling differences in sampling (e.g., spatial scales) between Aquarius data (averaged over Aquarius footprint) and the point-wise-in-situ measurements. For further discussions about the uncertainties in Aquarius Salinity, the readers can refer to the memo of "Assessment of Uncertainties in Aquarius Salinity Retrievals AQ-014-PS-0021" by Thomas Meissner (Remote Sensing Systems). Random and systematic uncertainties have been added to the Level 3 monthly data, as well.

Here we use 31 months of data (from September 2011 to March 2014, when V2.0 processing stopped) for V2.0 data and 45 months of data from V3.0 to V5.0 (the whole mission period from September 2011 to May 2015) for validation analysis. The rain flag is included only in V5.0, but here we applied the rain flag to both V4.0 and V5.0 for better comparisons.

Although considerable improvements have been achieved since V2.0, there remain a number of issues affecting the quality of the V5.0 data. These are detailed in the report and summarized in the last section (**Summary, Conclusions and Cautions).**

Readers of this document are assumed to be familiar with the Aquarius/SAC-D mission and sensor design, sampling pattern, salinity remote sensing principles, and pre-launch error analysis as described by [1] and [2]. It is particularly important to point out that the measurement sensitivity of L-band brightness temperature to salinity reduces from the tropics (relatively high sea surface temperature, SST) to high-latitude oceans (relatively low SST). As a result, L-band salinity data such as those from Aquarius are more prone to errors in the high latitudes than in the tropics. This information is documented in the ATBD document [3].

The sensor calibration is done with a forward model to estimate the antenna temperature at the satellite, then differencing that estimate from the measured antenna temperature on a global average [4]. The forward model includes the surface emission, geophysical corrections, antenna pattern correction, etc. This has removed the quasi-monthly, non-monotonic, variations previously seen in the V1.3 data.

The surface emission for the forward model is derived from ancillary SST and SSS. Until V4.0, the SST data are derived from the daily high-resolution blended SST produced by NOAA National Center for Environmental Prediction (NCEP) as described in [5]. In V5.0, The source of the ancillary sea surface temperature (SST) field has been

changed from the NOAA OI SST to the SST field from the Canadian Meteorological Center (CMC) [6] that has an overall better quality in high latitudes. More details for the reference SST can be found in [3]. The ancillary SSS data have been derived from the US Navy HYbrid Coordinate Ocean Model (HYCOM) daily averaged data-assimilative analysis ([7] and Appendix A). The operational data are produced by the U.S. Naval Oceanographic Office (NAVO), and the digital output is distributed by Florida State University. The HYCOM global mean salinity has been used as a surface calibration target for the sensor until V4.0. In V5.0 the reference SSS field that is used in the sensor calibration and in the derivation of TA expected (i.e. forward algorithm) has been changed from HYCOM SSS to the analyzed monthly Scripps Argo SSS (http://www.argo.ucsd.edu/Gridded_fields.html).

The Aquarius project produces three data sets: Level 1a (raw data), Level 2 (science data in swath coordinates and matching ancillary data), and Level 3 (gridded 1-degree daily, weekly and monthly salinity and wind speed maps, as well as sea water density and spice). This validation analysis will start with Level 2 data evaluation followed by Level 3 on monthly and seasonal (3-month) averages. Salinity measurements are on the practical salinity scale (PSS-78), technically a dimensionless number, but in some figures labeled as practical salinity units (psu).

2. Matchup maps and differences

We start with global maps comparing the Aquarius Level 2 samples with near-surface *in situ* salinity data, including those from Argo floats from US Global Ocean Data Assimilation Experiment (GODAE, http://www.usgodae.org/argo/argo.html) and global tropical moored buoy array from Pacific Marine Environmental Laboratory (PMEL, http://www.pmel.noaa.gov/tao/data_deliv/) (Error! Reference source not found.). The shallowest sampling depths of the Argo data are generally 3-5 meters below the surface. The shallowest sampling depth of the tropical buoy array can be as shallow as 1 meter. Under most conditions (e.g., moderate to high winds) the surface ocean mixed layer extends much deeper, and the buoy provides an accurate measure of the 1-2 cm surface layer that emits the microwave signal seen by the satellite. However, under persistently rainy conditions (especially under low winds when vertical mixing is small), there are often vertical gradients between the surface and the buoy measurement depth. For each *in situ* observation, we search for the closest point of approach (CPA) from the Aquarius Level 2 (swath) data. The time window is ± 3.5 days to gather all *in situ* data within the 7-day orbit repeat cycle. The search radius is 75 km between the *in situ* location and the bore sight position of the Aquarius footprint. The Aquarius data are averaged over 11 samples (~100 km) centered on the match-up point (i.e. the CPA). Argo floats rise to the surface once every 10 days and remain at the surface for a few hours. The data are collected randomly at any time of the day.

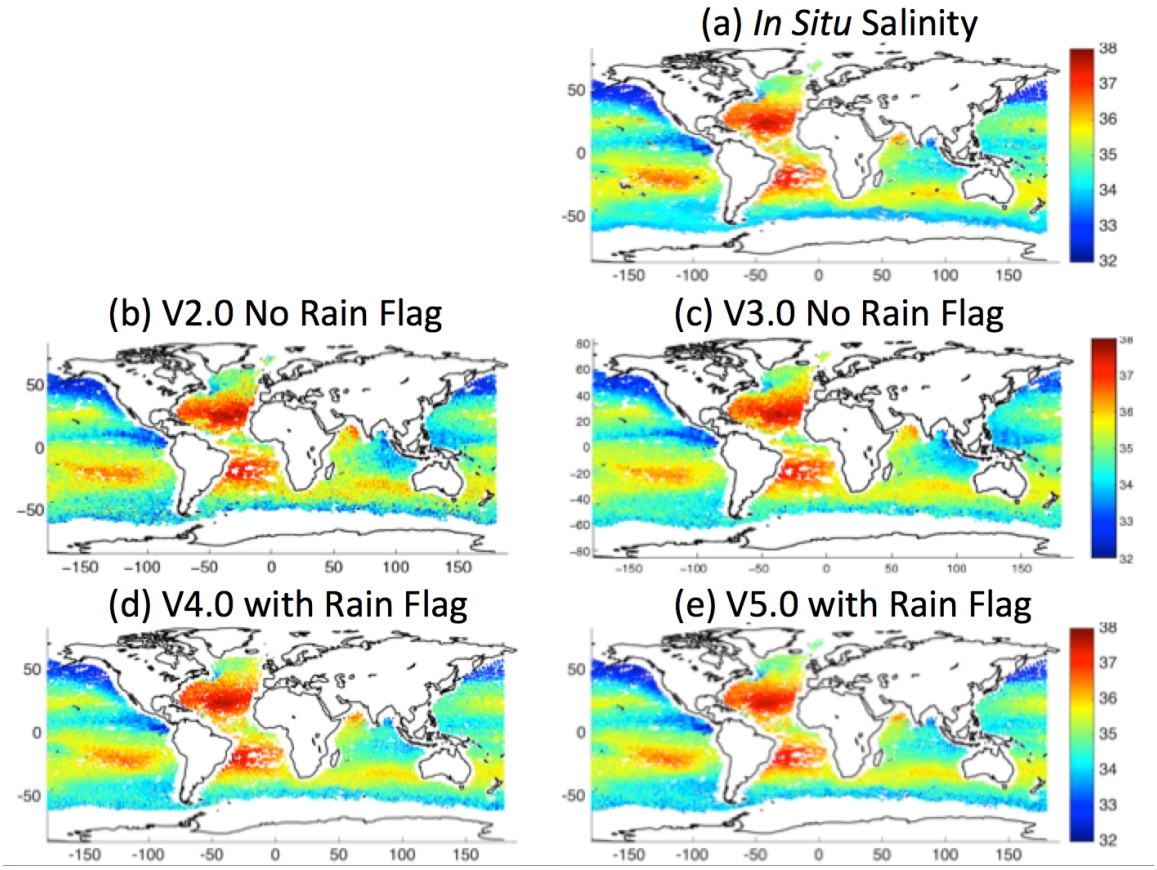

Figure 1. Aquarius and *in situ* co-located salinity data

Error! Reference source not found. shows the Aquarius retrieved salinity at the *in situ* matchup points for 31 months of V2.0 and 45 months of V3.0, V4.0 and V5.0 observations. *In situ* salinity data at the same matchup points are also shown. The correspondence is visibly quite clear with Aquarius Level 2 data resolving the salient large-scale ocean features. V2.0 data are somewhat noisier, especially in the extreme southern latitudes. The biases in the Southern Ocean are much reduced in V3.0 and V4.0 because of the improved roughness correction. In V3.0 and V4.0, Aquarius HHH winds are used to replace the NCEP winds, which are used in V2.0. In Aquarius V5.0, the bias adjustment for the global average is based on the SSS after the rain flag is applied, so the SSS in the Southern Ocean is fresher than V3.0 and V4.0 and is closer to the *in situ* value.

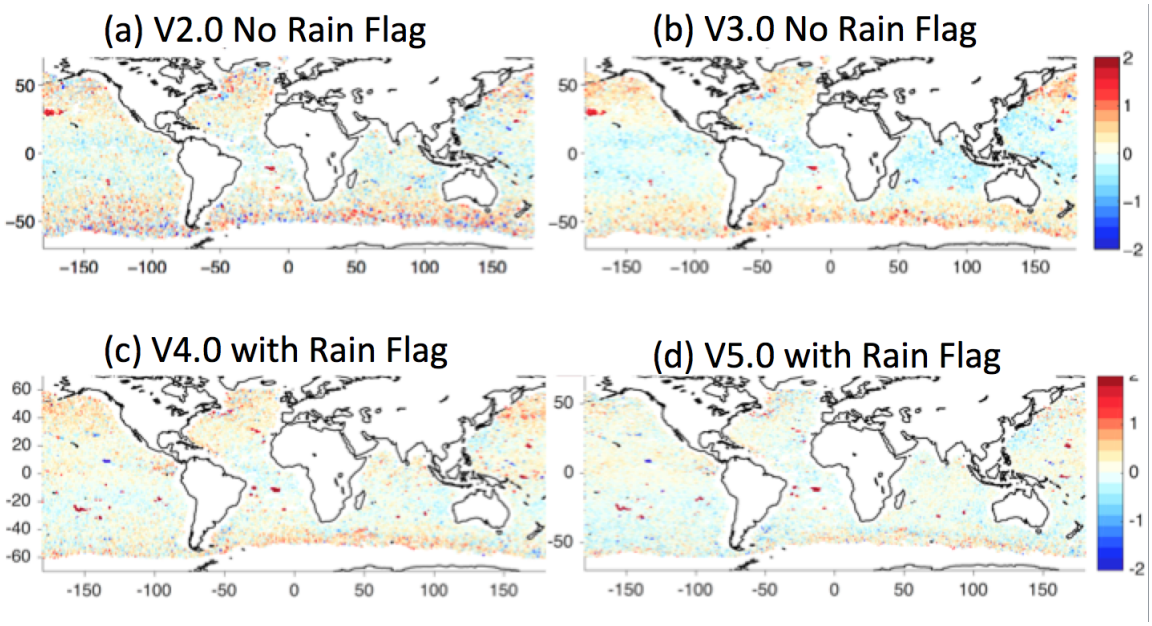

Figure 2. Global maps of SSS differences defined as the Aquarius (a) V2.0 (b) V3.0 (c) V4.0 and (d) V5.0 data minus the co-located *in situ* salinity.

Error! Reference source not found. shows the Aquarius – *in situ* differences with the same match-ups for V2.0, V3.0, V4.0 and V5.0. The noise in V2.0 in the Southern Ocean is reduced from V3.0 to V5.0. The latitudinal biases in V3.0 that appeared after the galaxy correction decreased in the later versions. Positive biases in V4.0 after applying the rain flags also decrease in V5.0. Other systematic improvements less visible here will be demonstrated by related analyses below.

3. 3-beam histograms

Histograms of the matchup salinity differences for each of the three beams are reported in **Figure 3**. In these statistics, we excluded the colocations that introduced considerable noise and skewness to the data (SST < 5°C, wind speed > 15 m/s, and gain-weighted land and ice fractions >0.001). There is a measureable improvement of the bias (median), and reductions in the standard deviations in all three beams. The root-mean-square difference (RMSD), which is the root sum square (RSS) of the bias and standard deviation, is reduced from ~**0.51** in V2.0, ~**0.44** in V3.0, ~**0.35** in V4.0 to ~**0.31** in V5.0. These are the ensemble statistics for the 31-month data for V2.0 and 45-month data for the other versions.

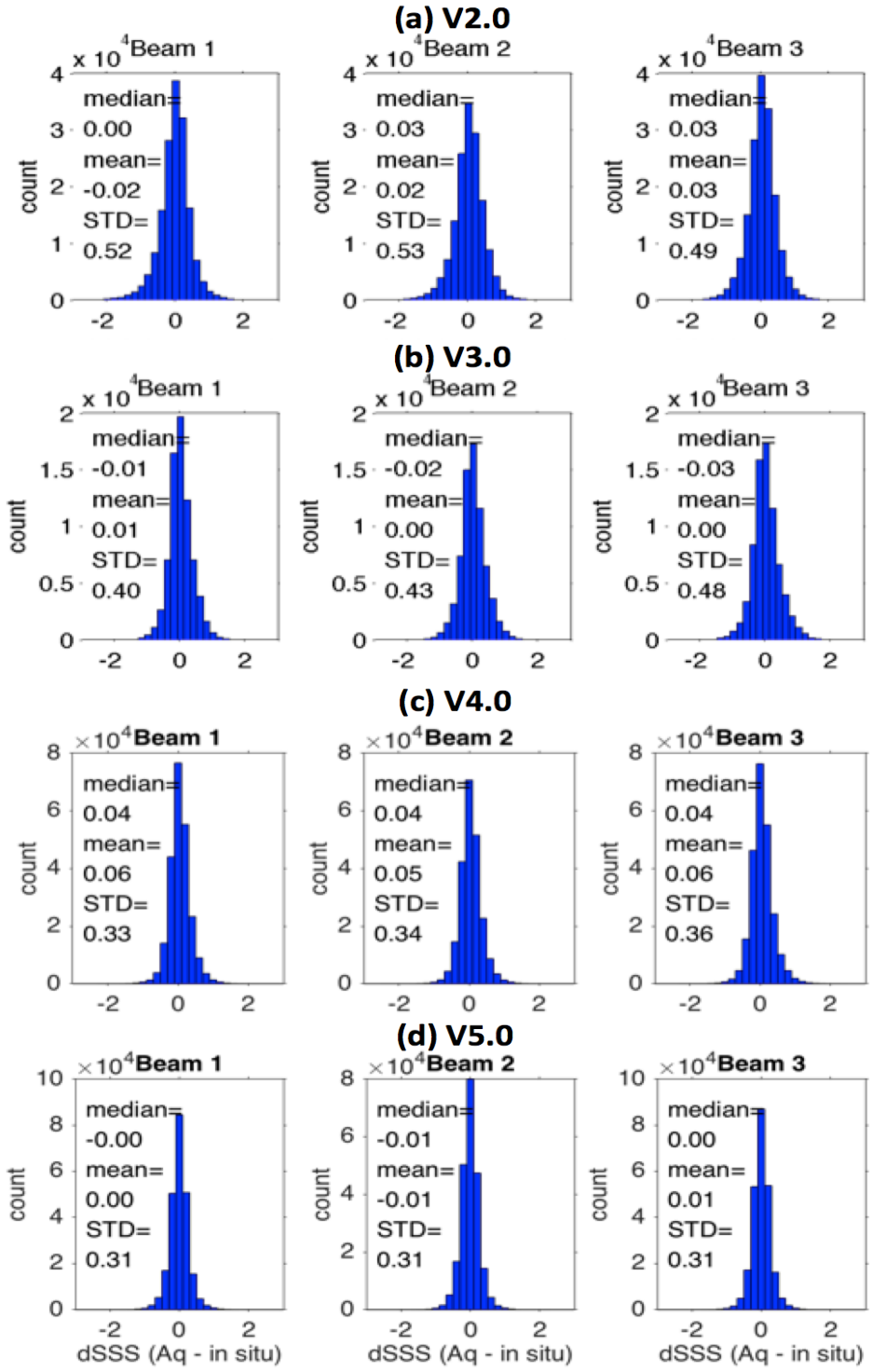

Figure 3. Histograms for Aquarius - in situ differences.

Scatter plots between the *in situ* data and each version of Aquarius data at the closest point of Aquarius (CPA) are shown for all three beams in **Figure 4**. The color contours represent the density of points, and fit is quite linear over the open ocean salinity dynamic range. Some outliers (faint yellow color) are evident with in situ salinity at about 34 psu, and these points are generally in the high latitudes. The lower surface temperature causes the lower sensitivity to the SSS and therefore larger biases. It is evident that Aquarius salinity observations are more concentrated to the 1:1: ratio line from version to version, indicating the smaller biases in V5.0. **Figure 4** also shows that he correlation coefficients between *in situ* and Aquarius data are ~0.87 in V2.0 and improve to ~0.94 in V5.0.

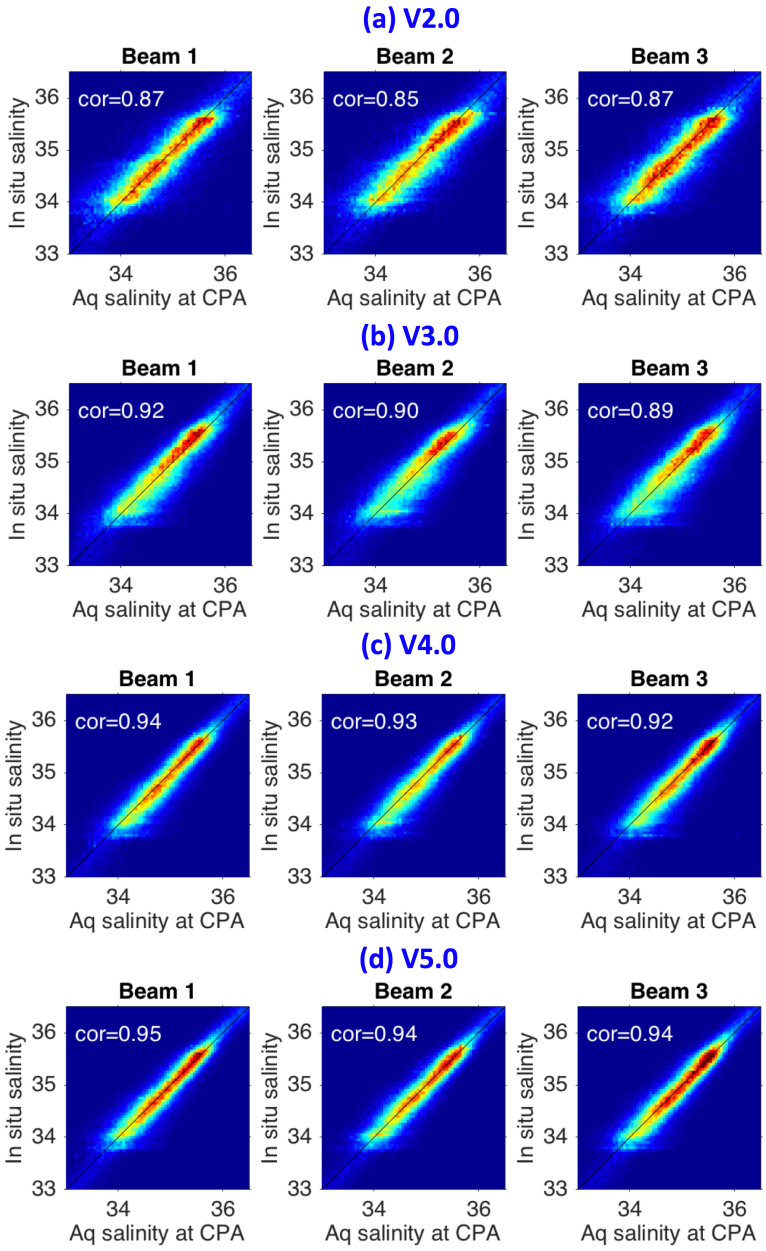

Figure 4. Scatter plots of *in situ* salinity (ordinate) and (a) V2.0 (b) V3.0 (c) V4.0 and (d) V5.0 Aquarius data at the closest point of Aquarius (CPA, abscissa) for each beam.

The HYCOM data are used as a salinity reference in Aquarius Level 2 data [4]. The HYCOM surface salinity is interpolated to the time and location of every 1.44 second sample interval. Here, in **Figure 5**, these reference salinity data are evaluated against the Argo measurements with the same matchup processing as Aquarius Level 2 data for the whole Aquarius mission time period. In other words, the HYCOM data are co-located and compared with the *in situ* data. The results are shown separately for the ascending (northward) and descending (southward) halves of the orbit. The first feature to emphasize is that there is no systematic difference between the ascending to the descending passes for the difference between *in situ* and HYCOM salinity. This equivalence indicates that the ascending – descending differences found in V2.0 are not realistic and have been greatly reduced in the later versions; comparisons are shown in **Section 7 & 8**. Secondly, it is clear that there are regional long-term systematic biases between HYCOM salinity and the *in situ* data. HYCOM is biased positively relative to the Argo floats in the Circumpolar current, tropics and North Pacific. Over much of the mid latitudes the bias is slightly negative. These differences exist even though most of the in situ data we are using here are assimilated by HYCOM and therefore not fully independent data.

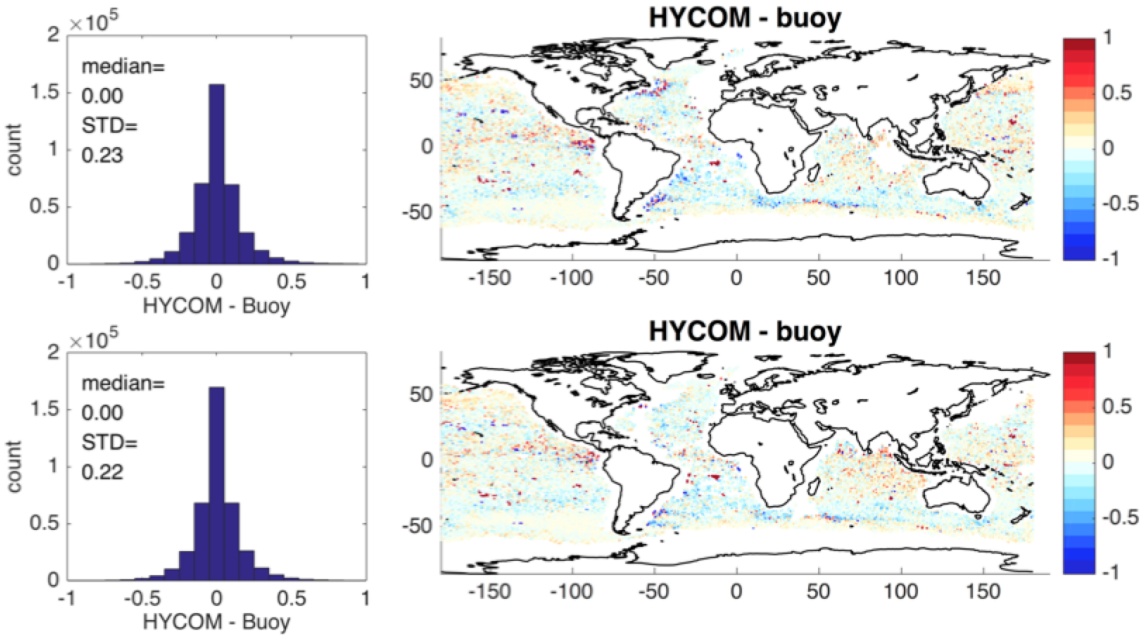

Figure 5. Salinity differences between co-located HYCOM and *in situ* for ascending (top) and descending (bottom) passes.

The histograms and statistics in **Figure 5** demonstrate that for the global average, the HYCOM-*in situ* differences have no bias, either for ascending or descending passes. This is a relevant point for validating our overall calibration approach because we used the HYCOM salinity as a surface reference for modeling the on-orbit antenna temperatures for calibrating the sensors in the earlier versions of Aquarius and we use Argo salinity for V5.0. We compute these calibrations on a global scale with running averages that use all orbits in a 7-day repeat cycle. In contrast, the HYCOM-*in situ* regional differences demonstrate that regional or zonal calibrations will be problematic, and we have used only global analyses for calibration. See also Section 12.2 below, Notes of Caution, regarding asymmetric RFI effects on ascending and descending maps.

4. Triple point analysis of Aquarius Level 2 data, HYCOM and *in situ* data

Figure 6 gives the V5.0 matchup statistics for Aquarius-*in situ*, HYCOM-*in situ*, and Aquarius-HYCOM (at the *in situ* locations), for each of the three beams. The results for earlier versions of Aquarius data can be found in the V2.0 and V4.0 validation documents. The root-mean-square deviation (RMSD) is defined as $RMSD=\sqrt{bias^2+STD^2}$. **Figure 6** shows HYCOM-*in situ* RMSD ~0.23 overall. The RMSD for Aquarius-*in situ* and Aquarius-HYCOM are 0.31 and 0.27, respectively. The co-located statistics allow us to estimate the root-mean-square error (RMSE) of each of the three measurements (*See Appendix B*). The results of V2.0 to V5.0 at beam 2 co-located matchup points are given in **Table 1**. The Aquarius RMSE are ~0.47 in V2.0, ~0.35 in V3.0, ~0.20 in V4.0 and ~0.17 in V5.0. The HYCOM and *in situ* RMSE are ~0.18 in V2.0 and V3.0 when the rain flags are not applied yet. HYCOM RMSE are reduced to ~0.09 and *in situ* RMSE are reduced to ~0.13 in V4.0 and V5.0 with the rain flag. Recall that these Aquarius matchup statistics are for individual match-ups, with no averaging. The idealized monthly average RMSE is possibly as low as ~0.17 for V2.0 and ~0.06 for V5.0, assuming a minimum of 8 samples per month and uncorrelated errors, as seen in the lower panel of **Table 1**. Directly computed monthly statistics are not this small, as will be discussed in a later section.

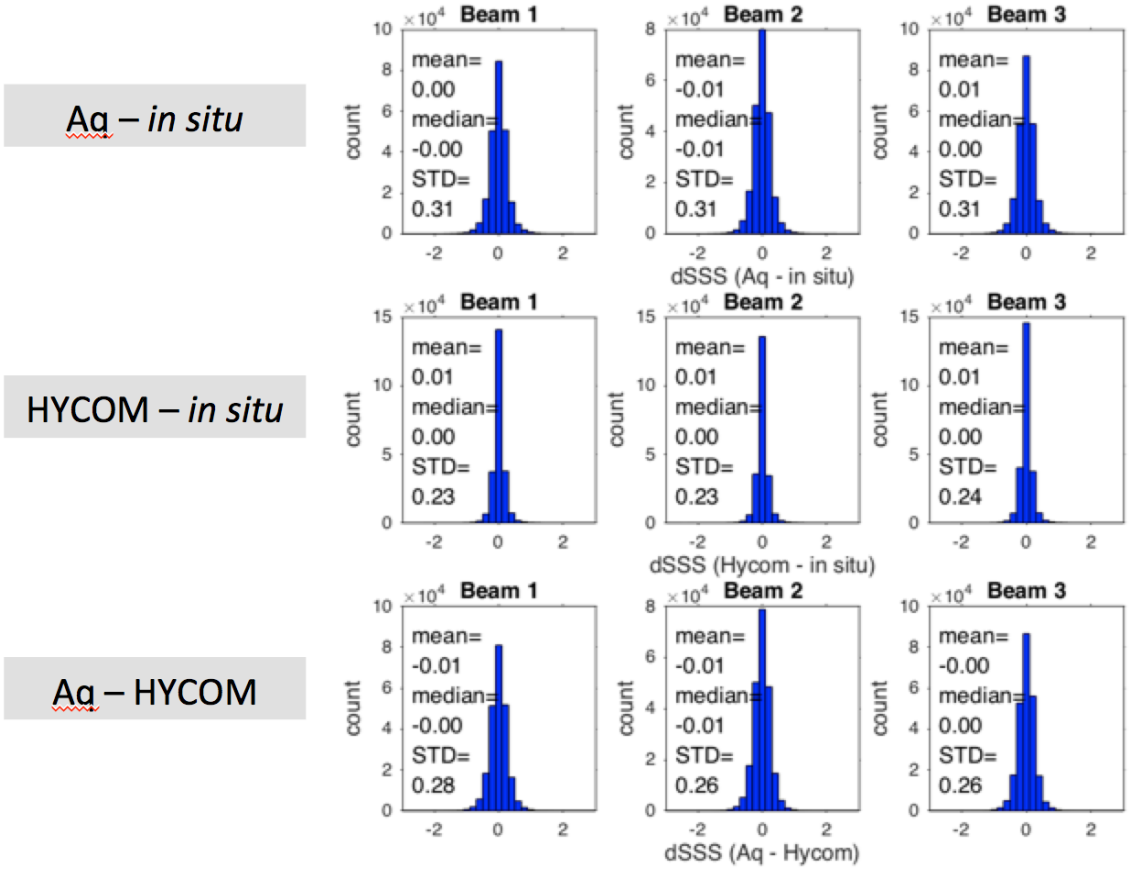

Figure 6. Co-located difference histograms for each beam of Aquarius V5.0 data. (top) Aquarius - *in situ*, (middle) HYCOM - *in situ*, (bottom) Aquarius - HYCOM.

Table 1. Estimated Root Mean Square Error (RMSE) for each data type based on the triple point analysis of beam 2 co-located point measurements.

Beam 2	V2.0	V3.0	V4.0	V5.0
Aquarius RMSE	0.47	0.35	0.20	0.17
HYCOM RMSE	0.18	0.16	0.09	0.08
In situ RMSE	0.18	0.18	0.13	0.14
Theoretical monthly RMSE if all errors are uncorrelated.				
Monthly RMSE psu (8 samples worst case)	0.17	0.12	0.07	0.06

5. *In situ* matchup time series

Figure 7 shows the global average salinity bias over time in Beam 2 for V2.0 to V5.0. The variations of the daily biases are similar in all three beams for each version, so only results in Beam 2 are shown here to demonstrate the progress throughout the different versions. Before V2.0, there are non-monotonic, quasi-monthly variations, which we often refer to as 'wiggles'. The issue has been resolved since V2.0 data with radiometer calibration adjustments. The small calibration drifts with near-annual time scale in V2.0 are effectively removed in V3.0 after the galaxy corrections. The updated flags in V4.0 also reduced the spikes in the time series. In V5.0, the slight positive bias and small variations in V4.0 are further improved.

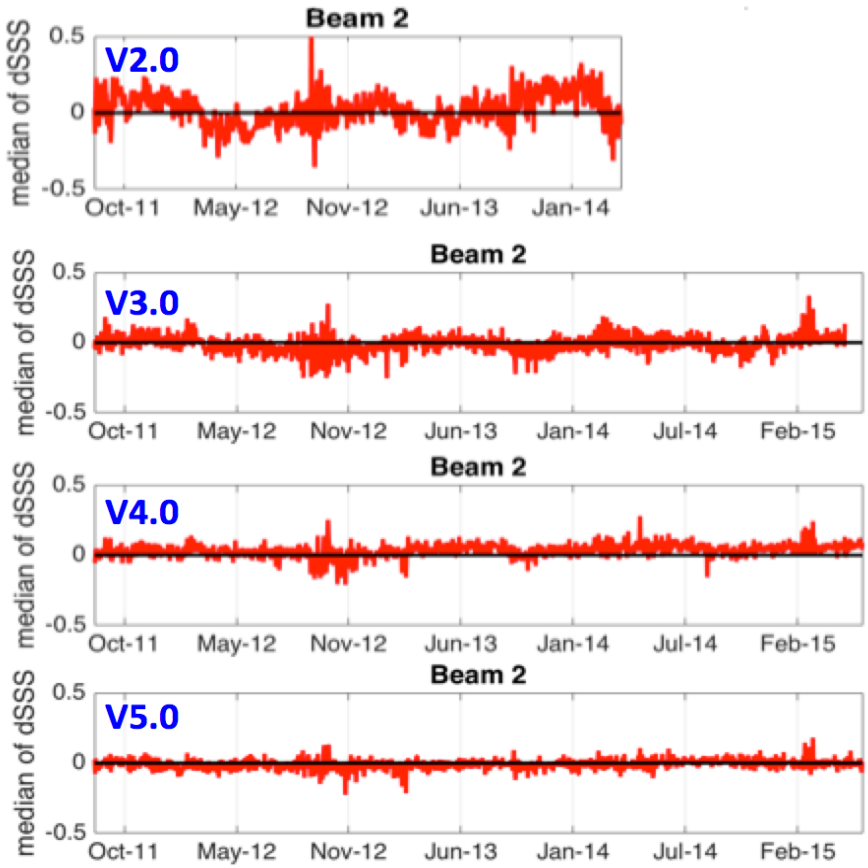

Figure 7. Daily global average Aquarius – *in situ* difference time series in beam 2 from V2.0, V3.0, V4.0 to V5.0.

Figure 8 shows the time series of daily differences between *in situ* and Aquarius V5.0 in three beams. All three beams show small differences with almost no variations. The remaining differences may be related to the uncertainties of salinity observations, such as near-surface stratification or the sub-footprint variations. The spikes in the figures happen when there are only insufficient matchup points on the day to average out the anomalous matchup results.

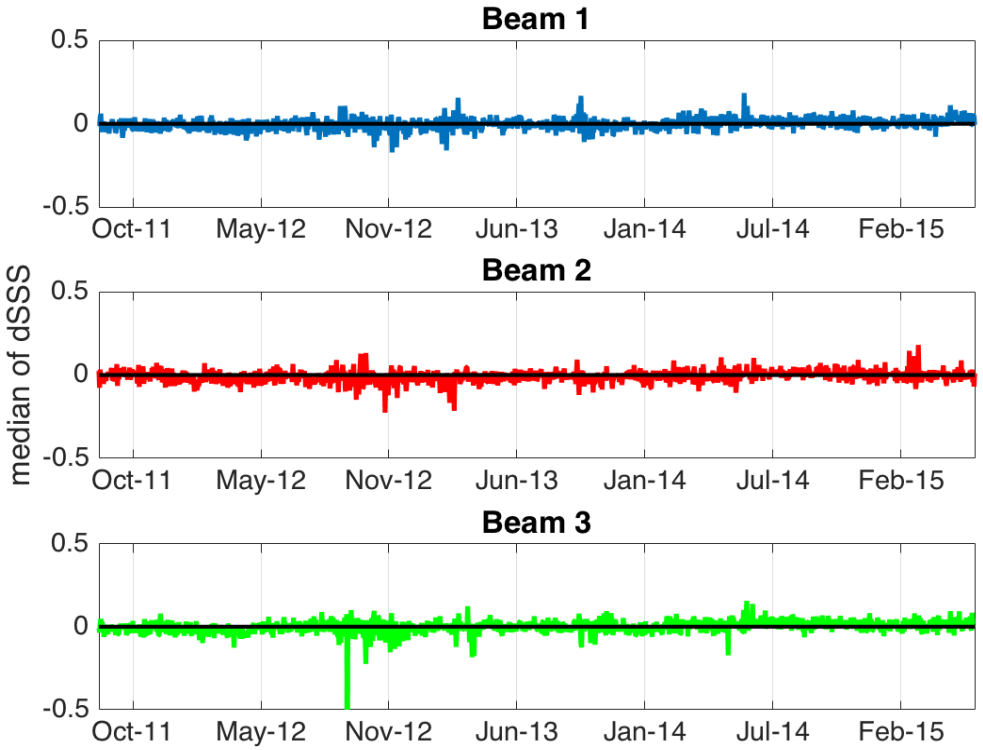

Figure 8. Time series of daily differences between *in situ* data and Aquarius V5.0 in three beams.

6. Monthly *in situ* matchup

Next, we examine *in situ* difference statistics of monthly 1x1 degree Level 3 salinity data maps. The Level 3 maps are generated from Level 2 salinity data without any added adjustment for climatology, reference model output or *in situ* data. The smoothing interpolation applies a bi-linear fit within a specified search radius. The standard Aquarius Level 3 data produced by the Aquarius Data Processing System (ADPS) use the criterion for land fraction set as 0.01 (severe) to include more salinity information near the coastal regions. As a result, the standard deviations are much higher compared to the gridding using 0.001 (moderate) for land fraction. *Therefore, when using the ADPS L3 mapped data, the users should be careful when analyzing the salinity data near the coasts.* For additional information see Section 4.2 Aquarius Flags in Aquarius Level-2 Data Product AQ-014-PS-0018. More details about the biases in the monthly maps will be discussed in **Figure 9**. Most of the results shown here are computed using a ~150 km radius. The radius is longer than what we used for Level 2, which is 75 km, to obtain more matchup with the *in situ* data and to average out the daily variations. The ADPS L3 data used in this document is filtered with rain masks and the data files are labeled as "*RAIN_MASK_SSS_1deg".

6.1 Aquarius – in situ monthly difference statistics

Table 2. V5.0 Aquarius-*insitu* monthly difference statistics (L3 maps from Aquarius Data Processing System with rain masks). Each panel represents one year (Sep-Aug) beginning Sep 2011.

	Aq-*insitu*	
	BIAS	STD
Sep-11	-0.023	0.156
Oct-11	-0.006	0.172
Nov-11	-0.024	0.194
Dec-11	-0.024	0.172
Jan-12	-0.024	0.179
Feb-12	-0.025	0.18
Mar-12	-0.027	0.175
Apr-12	-0.029	0.173
May-12	-0.016	0.188
Jun-12	-0.001	0.175
Jul-12	-0.017	0.155
Aug-12	-0.021	0.157

	Aq-*insitu*	
	BIAS	STD
Sep-12	-0.016	0.168
Oct-12	-0.006	0.196
Nov-12	-0.014	0.217
Dec-12	-0.021	0.173
Jan-13	-0.016	0.154
Feb-13	-0.006	0.154
Mar-13	-0.009	0.157
Apr-13	-0.017	0.156
May-13	-0.01	0.168
Jun-13	-0.012	0.216
Jul-13	-0.01	0.184
Aug-13	-0.02	0.171

	Aq-*insitu*	
	BIAS	STD
Sep-13	-0.007	0.17
Oct-13	-0.009	0.163
Nov-13	-0.023	0.159
Dec-13	-0.031	0.172
Jan-14	-0.019	0.176
Feb-14	-0.015	0.251
Mar-14	-0.011	0.221
Apr-14	-0.015	0.247
May-14	0.003	0.228
Jun-14	-0.002	0.229
Jul-14	0.003	0.234
Aug-14	0.012	0.237

Table 2. Continued

	Aq-*insitu*	
	BIAS	STD
Sep-14	0.025	0.218
Oct-14	0.012	0.21
Nov-14	0.007	0.235
Dec-14	-0.004	0.26
Jan-15	-0.002	0.229
Feb-15	-0.002	0.215
Mar-15	0.002	0.277
Apr-15	0.002	0.22
May-15	0.007	0.242

Table 2 shows the results of Level 3 monthly validation for V5.0 and the monthly *in situ* matchup maps are shown in **Figure 9**. The tabulated monthly standard deviations range from 0.154 to 0.277 from Sep 2011 to May 2015.

6.2 Global maps of salinity monthly biases

The maps of Aquarius V5.0 monthly biases for the first year of observations (September 2011 to August 2012) are shown in **Figure 9**. Positive biases are observed in the Southern Ocean near the Indian Ocean and the Pacific Ocean salinity peak in October and November. Negative biases are observed in the northeastern Atlantic above 60°N in February and on the both sides of Japan from October to May. The table shows consistent negative global mean bias for the months November through February.

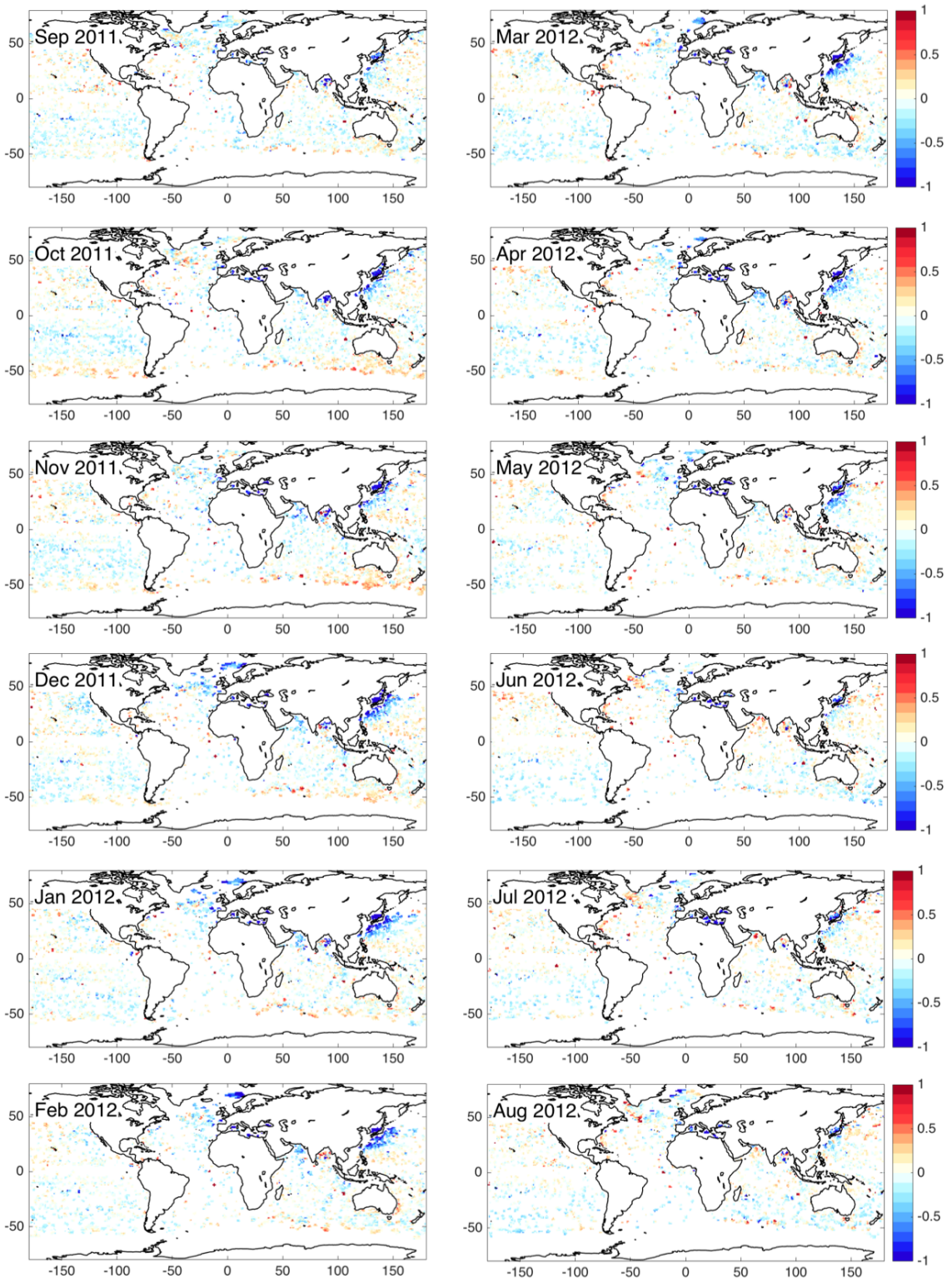

Figure 9. Aquarius V5.0 monthly difference maps (ADPS with rain masks).

6.3 Latitudinal variations of the salinity biases

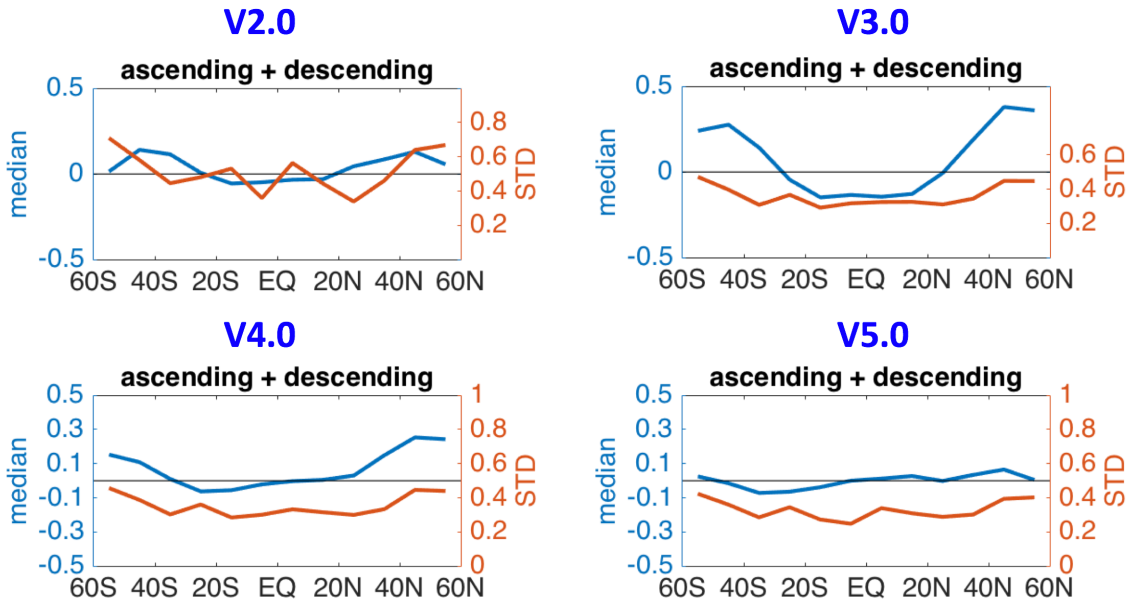

Figure 10. Differences of Aquarius gridded data (L3) and *in situ* salinity by latitude bands.

Figure 10 shows the *in situ* difference statistics in discrete latitude bands for entire orbits from V2.0 to V5.0 data. V2.0 biases are slightly negative (~-0.05 psu) in the tropics and positive (~0.2 psu) at 40°S and 40°N. Standard deviations are lower in the tropics and higher in the high latitudes. The latitudinal biases that are obvious in V3.0 (**Figure 10** upper right) are significantly reduced in V4.0 with the updated geophysical model function (GMF) to correct SST and wind effect on roughness in V4.0. The standard deviations are about the same in V3.0 and V4.0. In V5.0, the positive biases are greatly reduced in high latitudes, which was seen in **Figure 2**.

6.4 Triple-Point Analysis of Monthly Level 3 Gridded Data

Here, we apply the triple-point approach (Appendix B) to assess the Aquarius monthly root mean square error (RMSE). Table 2, above, gives the month-by-month bias and standard deviation (STD) differences between the Aquarius monthly L3 gridded data and in situ observations. From these, the root mean square difference (RMSD) is obtained as the square-root of the ($bias^2$ + STD^2). The RMSD, of course, combines both the Aquarius and in situ measurement errors, whereas our goal here is to isolate the Aquarius RMSE.

Three data sets for the triple-point analysis are (1) the same monthly 1x1 degree Level 3 salinity data maps as above in Section 6, (2) similarly gridded HYCOM SSS monthly

1x1 maps, and (3) the in situ data set (un-gridded). Next, we find the RMSD of three data pairs: (1) Aquarius-*in situ*, (2) HYCOM-*in situ*, and (3) Aquarius-HYCOM. The process finds all the *in situ* data points within the mapped 1x1 boxes for each month, averages those, differences that from the gridded monthly value for that grid-box, and then computes the RMSD of all the matched 1x1 grid-boxes over the globe for that month. Aquarius-HYCOM is simply the RMSD between the respective monthly 1x1 maps. The RMSD accumulations also ensure that only the 1x1 grid boxes containing in situ samples are counted, to ensure common sampling. We also note that the standard Level 3 gridding masks and flags are applied, and thus cold regions (SST<5°C) and regions higher than the threshold for land contamination are omitted (See Table 1 in AQ-014-PS-0018_AquariusLevel2specification_DatasetVersion5.0 for the description of data quality flags and masks).

The accumulated monthly biases and STDs are show in Table 3 for HYCOM-*in situ*, and Aquarius-HYCOM difference pairs (whereas Aquarius-*in situ* are given above in Table 2).

The difference statistics are quite similar in magnitude for the three pairs. The triple-point analyses giving estimated RMSE of each measurement system (Aquarius, HYCOM,

Table 3: Triple-point analysis: Monthly Bias and Standard Deviation (STD) differences for pairs HYCOM-*insitu* and Aquarius-HYCOM. Each panel represents one year (Sep-Aug) beginning Sep 2011. Difference statistics for the monthly Aquarius-*insitu* pair are in Table 2

	HYCOM-*insitu*		Aq-HYCOM	
	BIAS	STD	BIAS	STD
Sep-11	-0.011	0.184	-0.006	0.176
Oct-11	-0.007	0.176	0.013	0.186
Nov-11	-0.002	0.175	-0.003	0.173
Dec-11	-0.009	0.18	-0.017	0.163
Jan-12	0.008	0.175	-0.034	0.183
Feb-12	0.002	0.185	-0.029	0.188
Mar-12	0.005	0.178	-0.032	0.182
Apr-12	-0.004	0.154	-0.024	0.166
May-12	-0.002	0.163	-0.006	0.166
Jun-12	-0.001	0.163	-0.002	0.178
Jul-12	-0.007	0.16	-0.002	0.166
Aug-12	-0.003	0.176	-0.035	0.176

	HYCOM-*insitu*		Aq-HYCOM	
	BIAS	STD	BIAS	STD
Sep-12	0.006	0.202	-0.033	0.191
Oct-12	0.007	0.207	0.004	0.192
Nov-12	-0.005	0.243	-0.009	0.196
Dec-12	-0.012	0.179	-0.003	0.192
Jan-13	0.002	0.164	-0.009	0.183
Feb-13	0.003	0.152	-0.006	0.169
Mar-13	0.006	0.125	-0.022	0.144
Apr-13	0.002	0.117	-0.024	0.146
May-13	0.001	0.141	-0.016	0.136
Jun-13	0.008	0.165	-0.027	0.157
Jul-13	-0.002	0.147	-0.014	0.142
Aug-13	0.007	0.137	-0.031	0.146

	HYCOM-*insitu*		Aq-HYCOM	
	BIAS	STD	BIAS	STD
Sep-13	-0.006	0.15	-0.006	0.134
Oct-13	-0.011	0.098	0.013	0.153
Nov-13	-0.004	0.128	-0.014	0.146
Dec-13	-0.004	0.15	-0.023	0.153
Jan-14	-0.001	0.146	-0.012	0.145
Feb-14	-0.002	0.231	-0.016	0.163
Mar-14	0.001	0.191	-0.011	0.176
Apr-14	0.002	0.23	-0.011	0.171
May-14	0.011	0.222	-0.001	0.136
Jun-14	0.004	0.189	-0.006	0.157
Jul-14	0.002	0.21	-0.003	0.144
Aug-14	0	0.226	0	0.132

	HYCOM-*insitu*		Aq-HYCOM	
	BIAS	STD	BIAS	STD
Sep-14	-0.002	0.199	0.023	0.143
Oct-14	-0.001	0.182	0.021	0.157
Nov-14	0.004	0.207	0.002	0.153
Dec-14	0.003	0.225	-0.005	0.167
Jan-15	0.006	0.187	-0.006	0.154
Feb-15	0.004	0.188	-0.014	0.152
Mar-15	-0.001	0.248	-0.007	0.152
Apr-15	0	0.186	0.001	0.153
May-15	0.01	0.216	0.001	0.143

in situ) are presented in Table 4. Note that the largest RMSE belongs to the *in situ* data. These are a combination of *in situ* sensor and representativeness errors. The latter include spatial and temporal variations of the *in situ* observations within the 1x1 grid box during the month, plus the salinity differences between the *in situ* sampling depths and the surface.

The Aquarius monthly RMSE estimates are <0.2 psu for all months of the mission, and the average over all months is 0.128. Given that 0.20 is the mission accuracy requirement for monthly average maps, this calculation verifies that the Aquarius data exceed the mission requirement by a substantial margin.

Table 4: Triple-point analysis: Monthly Root Mean Square Error (RMSE) differences for Aquarius, HYCOM and *insitu* fields. Each panel represents one year (Sep-Aug) beginning Sep 2011. At the bottom of the fourth panel, green highlight, are the average RMSE over the 45 months. Note that the Aquarius mean value is 0.128 PSU.

	Aquarius		HYCOM		In situ	
	MSE	RMSE	MSE	RMSE	MSE	RMSE
Sep-11	0.011	0.105	0.020	0.142	0.014	0.118
Oct-11	0.017	0.129	0.018	0.134	0.013	0.114
Nov-11	0.019	0.137	0.011	0.106	0.019	0.139
Dec-11	0.012	0.111	0.015	0.121	0.018	0.134
Jan-12	0.018	0.135	0.016	0.128	0.014	0.120
Feb-12	0.017	0.132	0.019	0.137	0.016	0.125
Mar-12	0.017	0.130	0.017	0.131	0.014	0.120
Apr-12	0.018	0.133	0.011	0.103	0.013	0.115
May-12	0.018	0.135	0.009	0.096	0.017	0.131
Jun-12	0.018	0.134	0.014	0.118	0.013	0.113
Jul-12	0.013	0.115	0.014	0.120	0.011	0.106
Aug-12	0.013	0.115	0.019	0.138	0.012	0.109

	Aquarius		HYCOM		In situ	
	MSE	RMSE	MSE	RMSE	MSE	RMSE
Sep-12	0.013	0.112	0.025	0.158	0.016	0.126
Oct-12	0.016	0.127	0.021	0.144	0.022	0.149
Nov-12	0.013	0.116	0.025	0.159	0.034	0.184
Dec-12	0.018	0.132	0.019	0.139	0.013	0.113
Jan-13	0.015	0.124	0.018	0.135	0.009	0.093
Feb-13	0.015	0.121	0.014	0.118	0.009	0.096
Mar-13	0.015	0.123	0.006	0.078	0.010	0.098
Apr-13	0.016	0.128	0.005	0.074	0.008	0.091
May-13	0.014	0.117	0.005	0.072	0.015	0.121
Jun-13	0.022	0.150	0.003	0.054	0.024	0.156
Jul-13	0.016	0.128	0.004	0.063	0.018	0.133
Aug-13	0.017	0.129	0.006	0.076	0.013	0.114

	Aquarius		HYCOM		In situ	
	MSE	RMSE	MSE	RMSE	MSE	RMSE
Sep-13	0.012	0.110	0.006	0.076	0.017	0.129
Oct-13	0.020	0.142	0.003	0.058	0.006	0.080
Nov-13	0.015	0.124	0.006	0.078	0.010	0.102
Dec-13	0.016	0.126	0.008	0.089	0.015	0.121
Jan-14	0.016	0.125	0.006	0.075	0.016	0.125
Feb-14	0.018	0.135	0.008	0.092	0.045	0.212
Mar-14	0.022	0.148	0.009	0.096	0.027	0.165
Apr-14	0.019	0.137	0.011	0.103	0.042	0.206
May-14	0.011	0.103	0.008	0.089	0.041	0.204
Jun-14	0.021	0.144	0.004	0.063	0.032	0.178
Jul-14	0.016	0.125	0.005	0.071	0.039	0.198
Aug-14	0.011	0.106	0.006	0.078	0.045	0.212

	Aquarius		HYCOM		In situ	
	MSE	RMSE	MSE	RMSE	MSE	RMSE
Sep-14	0.015	0.121	0.006	0.079	0.033	0.183
Oct-14	0.018	0.135	0.007	0.084	0.026	0.162
Nov-14	0.018	0.134	0.006	0.074	0.037	0.193
Dec-14	0.022	0.150	0.005	0.074	0.045	0.213
Jan-15	0.021	0.144	0.003	0.056	0.032	0.178
Feb-15	0.017	0.131	0.006	0.079	0.029	0.171
Mar-15	0.019	0.139	0.004	0.063	0.058	0.240
Apr-15	0.019	0.136	0.005	0.069	0.030	0.173
May-15	0.016	0.127	0.004	0.066	0.042	0.206

Mean RMS Values	0.128	0.097	0.146

7. Contrasting Ascending and Descending passes

We now examine the differences of SSS between the ascending (northward, 6pm) and descending (southward, 6am) orbits. In principle, the ascending and descending maps are expected to be nearly identical (e.g. **Figure 5**). **Figure 11** shows several residual modeling issues in the V2.0 data and the improvement of V5.0 data. Here we use a 31-month block of data from September 2011 through March 2014 for V2.0. The ascending-descending map for V2.0 shows several areas of concern with biases much in excess of 0.2 psu. In the Northern Hemisphere, a large blue patch in the eastern Atlantic, and red zones in the western Atlantic and Asian Pacific are believed to be related to low-level radio frequency interference (RFI) from adjacent land areas that is not detected by the standard RFI filter algorithm. This causes a positive brightness temperature bias and thus a negative salinity bias. The RFI asymmetry between ascending and descending is the results of the opposite viewing angle (toward or away from the land emitting sources) between the two sides of the orbit. The antenna faces eastward on ascending passes and westward on descending passes. The Southern Hemisphere biases are likely to be related to the galaxy reflection term that is not correctly adjusted for wind.

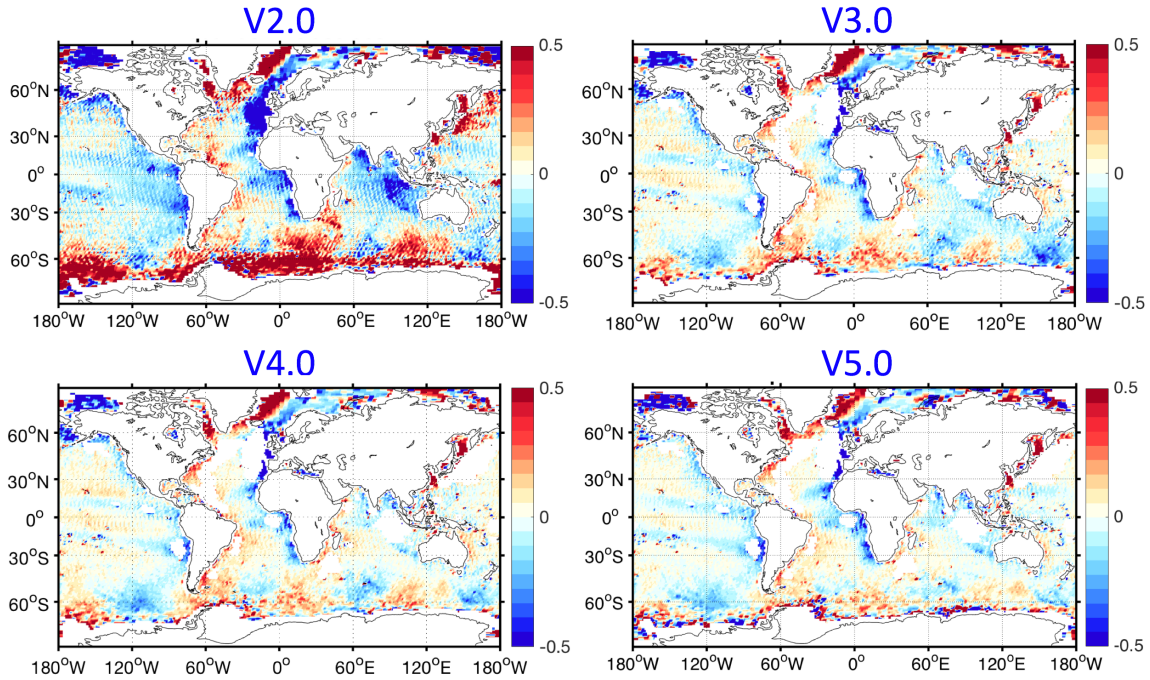

Figure 11. 31-month (V2.0) and 45-month (V3.0, V4.0 and V5.0) average averaged Ascending – Descending data. Major bias regions are described in the text. The "white" regions in the North Atlantic, Western Pacific (China, Japan) or Indonesia are masked out due to suspected undetected RFI. See flagging/masking tables in [9] for details.

Figure 11 also shows that in V5.0 the RFI influenced areas, including the both sides of the Atlantic Ocean, eastern Indian Ocean, and the northwestern Pacific are masked out for the large ascending minus descending biases. [Note that beginning with Aquarius data V3.0, regions with excessive asc-dsc differences due to RFI are masked when mapping, This shows gaps in the maps of only ascending or only descending passes. The ascending masked regions differ from the descending ones, and do not overlap. See AQ-014-PS-0006_ProposalForFlags&Masks_DatasetVersion3.0, which is included in the Data Version V5.0 documentation.] The biases in the extreme Northern Hemisphere are essentially unchanged. The positive biases (>0.5 psu) in the Southern Ocean for V2.0 have been significantly reduced in V5.0 (<0.2 psu) after improving the galaxy correction. There are visible asc-dsc biases at high southern latitudes that remain in V5.0. One can see a zonal variation between light blue and light red blobs around 60°S. It is not clear at this point what the reasons are for these asc-dsc biases.

8. Ascending – descending bias variations over time

Figures 12 contrasts the variability in time in V2.0, V3.0, V4.0 and V5.0 of the ascending-descending difference of the global average difference between Aquarius salinity and the *in situ* measurements. The variations of the differences are similar in all three beams (See Aquarius V2.0 and V4.0 validation documents and **Figure 13**), so only the results for beam 2 are shown here. It is evident that seasonal variations of the ascending and descending differences of up to ±0.5 psu are present in V2.0. The improved galaxy correction in V3.0 successfully removes the seasonal variations. The remaining ascending and descending differences are observed up to ±0.3 psu in certain time period. More positive differences show up in the earlier part of the mission and negative differences in the later part of the mission. The differences are reduced in V4.0 and even less than ±0.1 psu in V5.0.

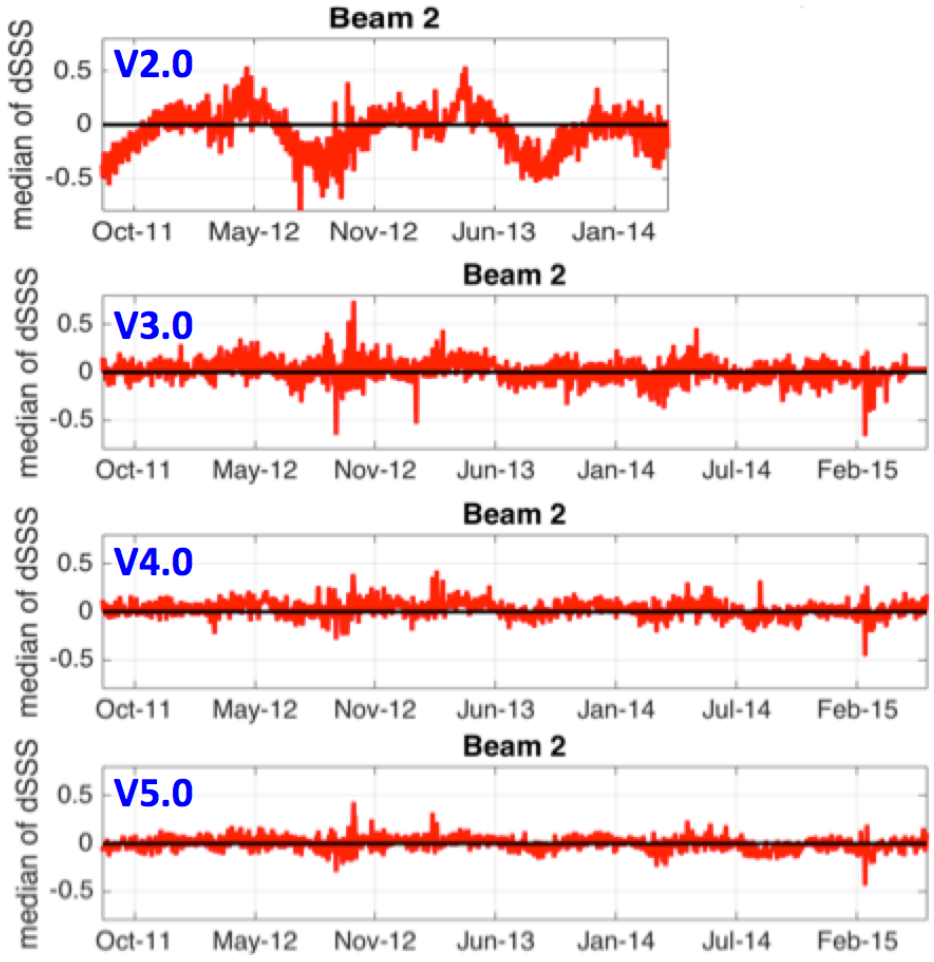

Figure 12. Daily average ascending minus descending Aquarius – *in situ* difference time series in Beam 2 from V2.0 to V5.0.

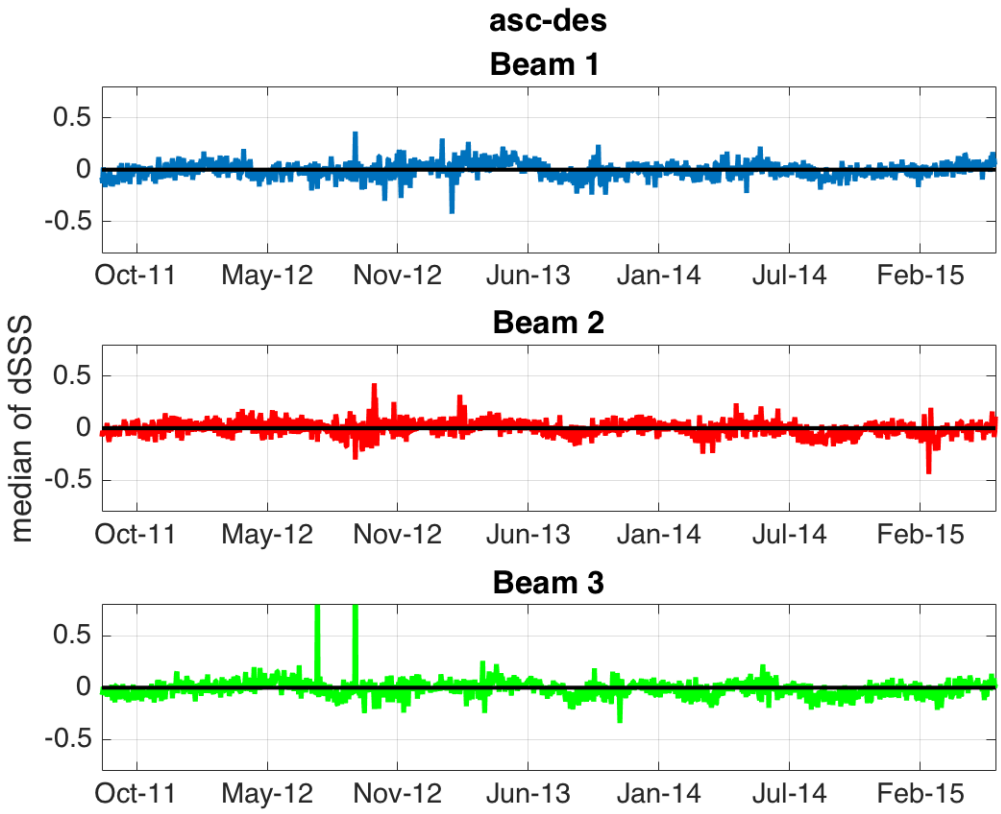

Figure 13. Daily average ascending minus descending Aquarius - *in situ* difference time series for all three beams of Aquarius V5.0.

Figure 13 shows that the annual variability of ascending minus descending differences in V5.0. Very small (< 0.1 psu) variations are remaining in all three beams. The cause of the differences includes not only the different Aquarius biases along the ascending and descending tracks but also the uncertainties from the time differences when the ascending and descending orbit pass the same location.

Figure 14 illustrates the magnitude and geographic pattern of the seasonal ascending minus descending differences on a monthly basis for the first year of observations. Seasonal variations of the biases in the Southern Hemisphere are still observed with positive biases in March-April-May and negative biases in July-August-September. The Northern Hemisphere RFI zones described in **Figure 11** are still persistent year-round.

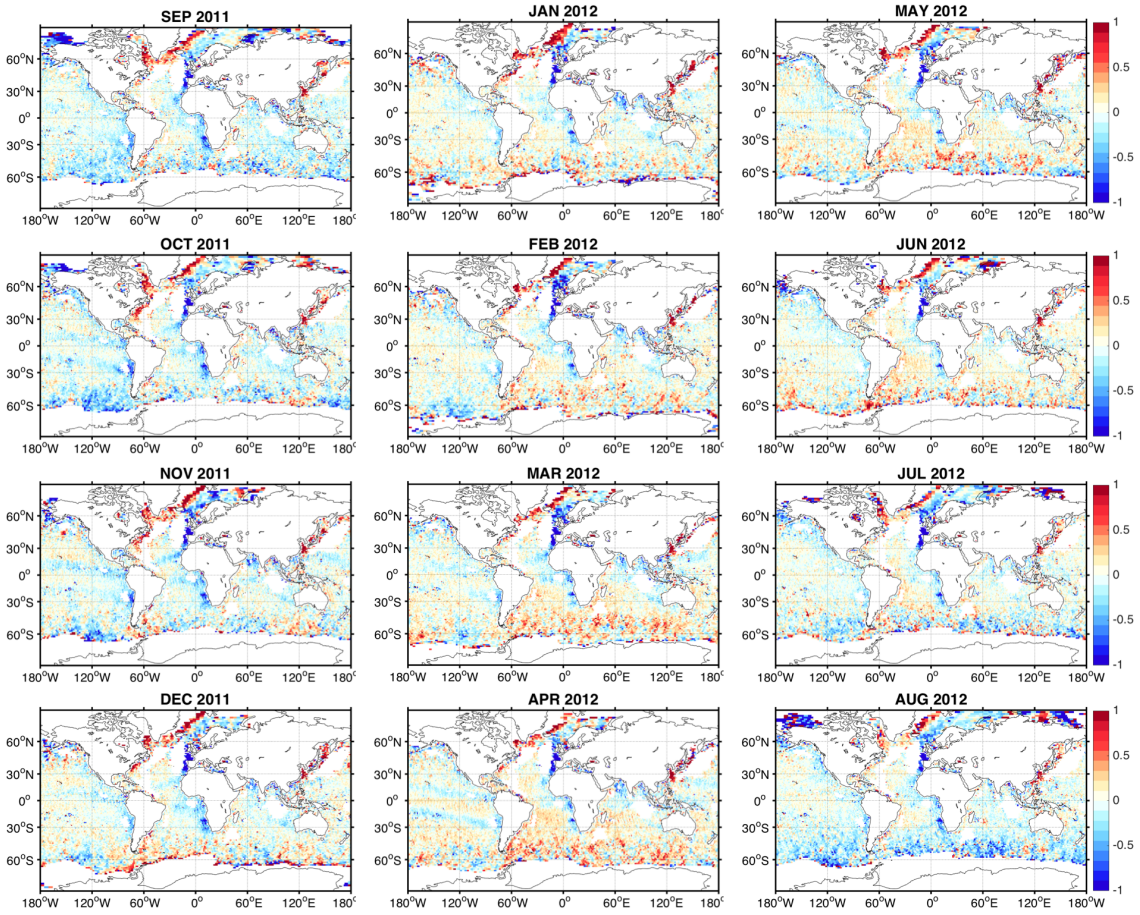

Figure 14. V5.0 ascending minus descending maps for September 2011 through August 2012 showing the seasonal progression.

9. Seasonally *in situ* matchup

This section shows the validation with *in situ* data for the L3 seasonal SSS maps. ADPS gridded maps with rain masks are used for analysis. When doing the validation, the *in situ* matchups are compiled for each 1-degree grid. All the *in situ* observations found within the 150 km radius within the same season of the Aquarius grid points are averaged to compare with the Aquarius data.

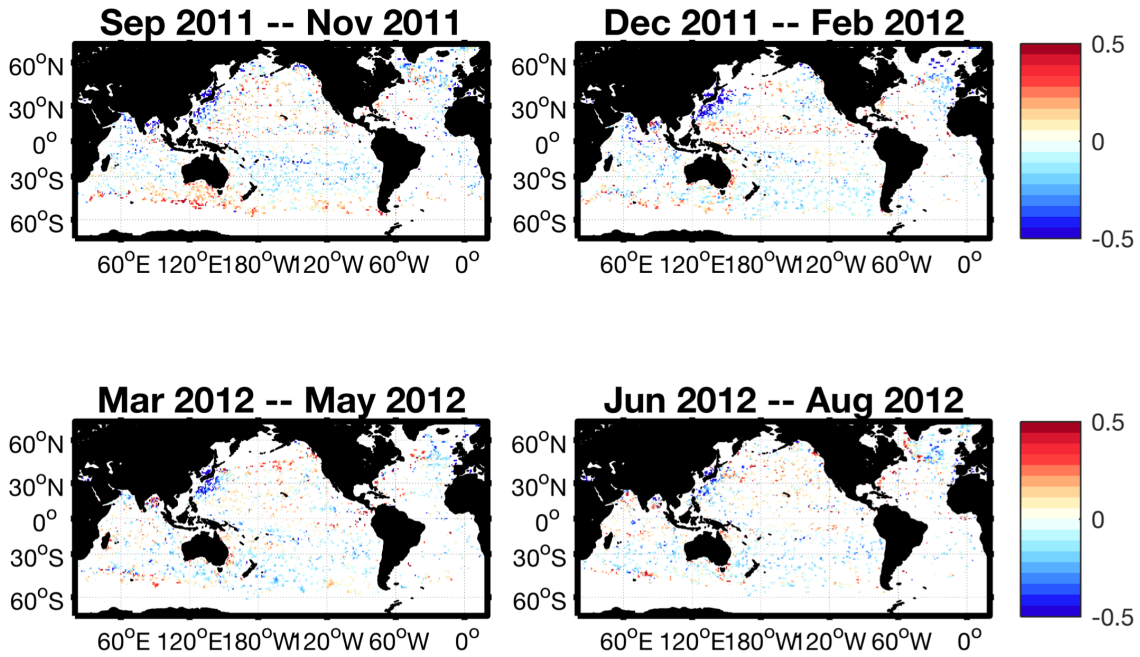

Figure 15. V5.0 Aquarius seasonal buoy difference maps in the first year of the observations.

Figure 15 shows the differences between Aquarius seasonal maps and the *in situ* average in the same time period. The differences may include the biases in Aquarius observation, vertical stratification and sub-footprint variations. The differences are generally < 0.2 psu in the open ocean. Large negative anomalies are observed near Japan from September to February and Positive values are seen in the Southern Ocean near the Indian Ocean in SON. These regions should be noted when the users are trying to analyze the seasonal variations of the Aquarius salinity data. **Figure 16** provides latitude distributions for the four seasons of Aquarius-*in situ* bias (blue) and standard deviations (red). In September-October-November the positive biases around 55°S correspond the biases in the Southern Ocean near Indian Ocean. In December-January-February, the positive biases around 30°S to 50°S correspond to the negative biases near Japan.

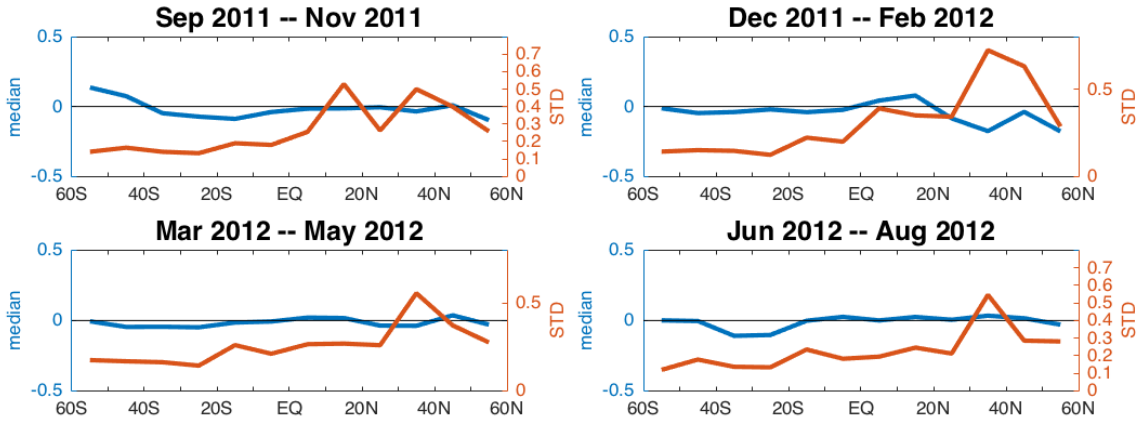

Figure 16. Seasonal average buoy differences by latitude range.

10. Evaluation of Aquarius level-3 SSS using Argo gridded products on various spatial scales from V3.0 to V5.0 (by Tong Lee from JPL)

The Aquarius SSS product used in the analysis are the Aquarius Version-3, 4, and 5, monthly 1°-gridded SSS (SCISM). Two Argo monthly 1°-gridded salinity products are used for comparison: one from the Scripps Institution of Oceanography (SIO) (http://www.argo.ucsd.edu/Gridded_fields.html) and the other one from the Asian Pacific Data Research Center of the University of Hawaii (UH) (http://apdrc.soest.hawaii.edu/projects/Argo/data/gridded/On_standard_levels/index-1.html). These two products, referred to as Argo-SIO and Argo-UH hereafter, have been widely used for scientific applications and for evaluating Aquarius SSS. The salinity field at the shallowest grid level of Argo-SIO (2.5 decibar, approximately 2.5 m) and the average of the two shallowest grid levels of Argo-UH (0 and 5 m) were extracted for analysis (referred to as Argo SSS hereafter). Aquarius measured salinity at the top centimeter of the ocean. Near-surface salinity stratification in the upper few meters can cause differences between Aquarius and Argo SSS, especially under rain bands.

Figure 17 shows the global average values of the regional root-mean-squared difference (RMSD) between Aquarius and Argo-SIO SSS for 1°x1°, 3°x3°, and 10°x10° scales for V3.0, V4.0, and V5.0. For all scales, there is a progressive reduction of the global RMSD value from V3.0 to V5.0. For example, for 1°x1°, the RMSD are 0.26 psu for V3.0, 0.21 psu for V4.0, to 0.18 psu for V5.0.

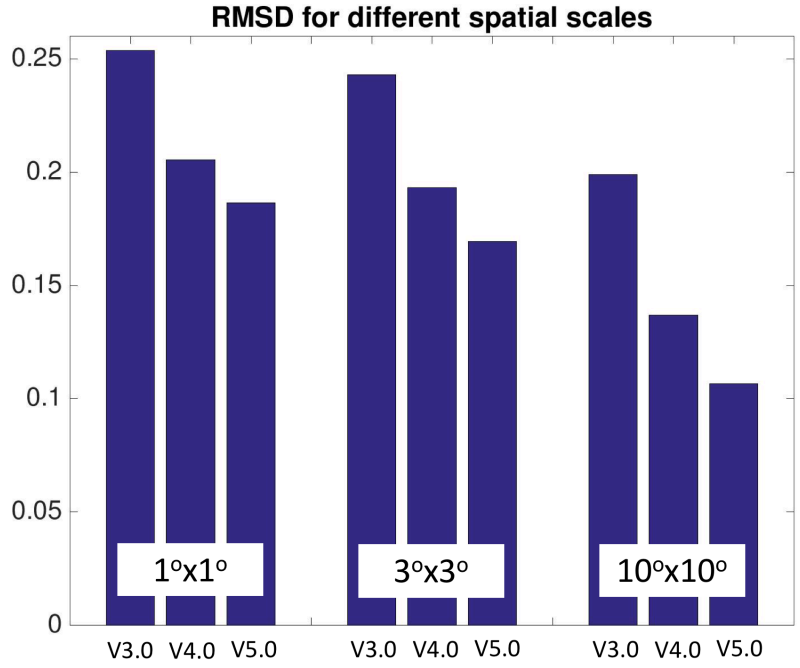

Figure 17. Global average values of the regional root-mean-squared difference (RMSD) between Aquarius and Argo-SIO SSS for 1°x1°, 3°x3°, and 10°x10° scales for V3.0, V4.0, and V5.0.

The RMSD values discussed above includes the contributions of differences in time mean values and differences for temporal anomalies (deviation from time mean) between Aquarius and Argo SSS. Many applications do not concern time mean biases but focus on variability (e.g., temporal and spatial changes). Therefore, we also assess the standard deviation (STD) of the differences between Aquarius and Argo SSS. The time-mean differences between Aquarius and Argo products do not contribute to the STD values as they do to the RMSD values.

Figure 18 shows the global averages of regional STD values of Aquarius SSS with respect to Argo-SIO SSS for various spatial scales from V3.0 to V5.0. The left column contains the STD values for total anomalies relative to the time mean differences. The middle column contains the STD values for seasonal anomalies, defined as the 3-year composite seasonal cycle during the Aquarius period (both for Aquarius and for Argo) relative to the 3-year time mean. The right column contains the STD values for non-seasonal anomalies, defined as the difference between the total anomalies and seasonal anomalies (e.g., intraseasonal and interannual anomalies). The STD for total anomalies on 1°x1° (left column of **Figure 18**) are significantly smaller than the RMSD values on the same scales (**Figure 17**) because the time mean differences between Aquarius and Argo SSS are not considered in the STD calculation. For total, seasonal, and non-seasonal anomalies, there is a consistent reduction of the STD values on all spatial scales from V3.0 to V5.0.

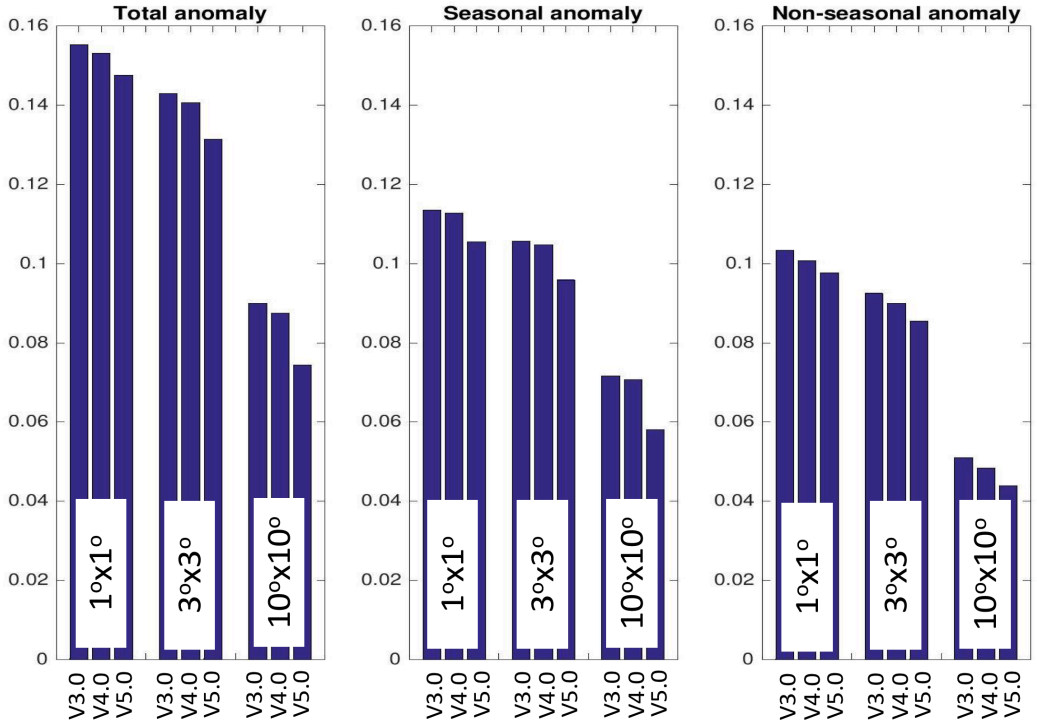

Figure 18. Global standard deviation (STD) values of Aquarius and Argo SSS for total anomaly (left), seasonal anomaly (middle), and non-seasonal (right) for various spatial scales from V3.0 to V5.0.

It is noteworthy that the global STD values for 10°x10° scale are approximately half of those for 1°x1° scale. Moreover, the STD values for seasonal anomalies are consistently larger than those for non-seasonal anomalies. To further examine the changes of seasonal biases from V3.0 to V5.0, **Figure 19** shows the latitudinal distribution of zonally averaged STD values for Aquarius-Argo SSS differences for seasonal anomalies. V5.0 is seen to have somewhat smaller seasonal biases with respect to Argo data then V3.0 and V4.0.

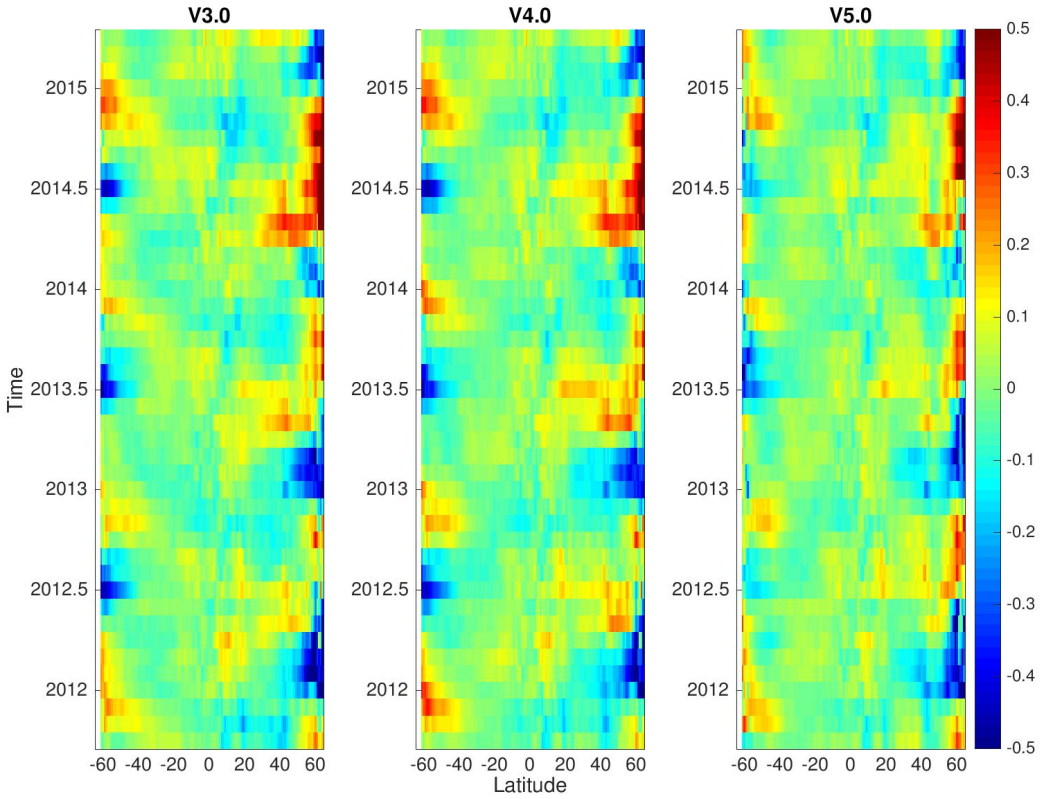

Figure 19. Latitudinal distribution of zonally averaged STD values for Aquarius-Argo SSS differences for seasonal anomalies.

The RMSD and STD values of Aquarius-Argo SSS differences are not only due to the uncertainty of Aquarius SSS, but also the uncertainty of the Argo gridded datasets as well. This is because Argo float distributions are too sparse to produce robust monthly mean values at 1°x1° scale in regions with strong spatiotemporal variability such as tropical rain bands (e.g., under the ITCZ), near river plumes, western boundary currents, and the Antarctic Circumpolar Current. High-resolution in-situ thermosalinograph (TSG) data indeed show significant variations of SSS within the scales of Aquarius footprint (Boutin et al. 2016). Therefore, the Argo gridded data in these regions can be significantly affected by the sampling errors of the Argo array. As fact, Lee (2016) found that the STD values between two of the Argo-SIO and Argo-UH products are as large or larger than the STD values between Aquarius and either of the Argo product in some of these regions. This is also reflected in **Figures 20** by comparing the STD maps for Aquarius-Argo salinity for

various versions of the Aquarius data as well as the STD for the difference between Argo-SIO and Argo-UH data. This issue also exists for the comparison of STD on 3°x3° scale (**Figure 21**). But for 10°x10° scale, Argo data have sufficient sampling to represent the large scale monthly mean values so the difference between the two Argo products are much smaller. The message for the comparison shown in **Figures 20** to **22** is that RMSD and STD values of the difference of Aquarius and Argo gridded data can be used as an indication of Aquarius data uncertainty, especially the change from one version to another. However, these values also contain the sampling uncertainty associated with the data products generated from the individual Argo profiles.

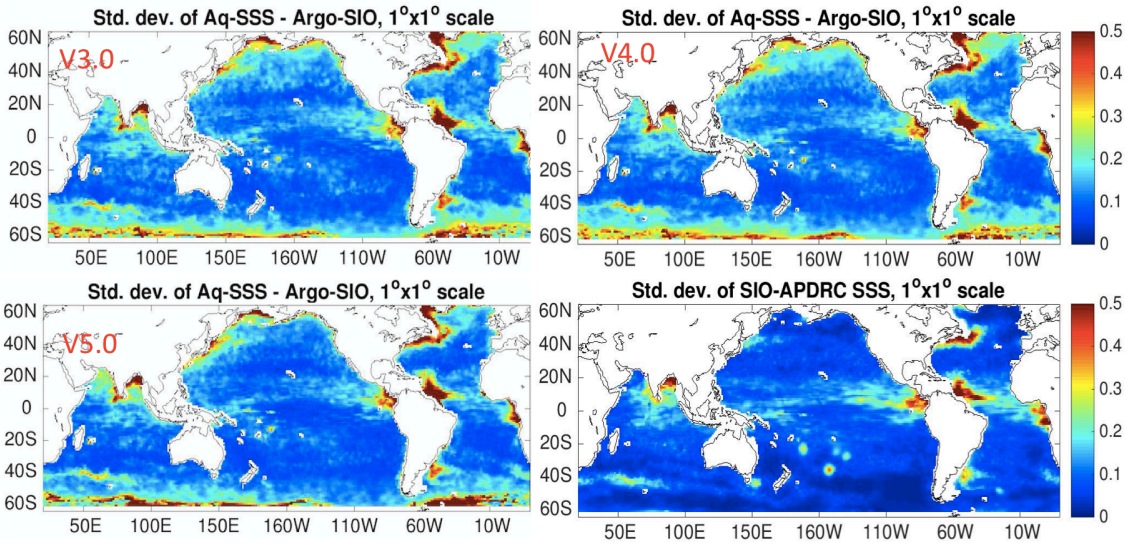

Figure 20. The STD of the difference between Aquarius and Argo-SIO SSS on 1°x1° scale for V3.0, V4.0, and V5.0. The STD of the difference between Argo-SIO and Argo-UH are shown in the lower right panel.

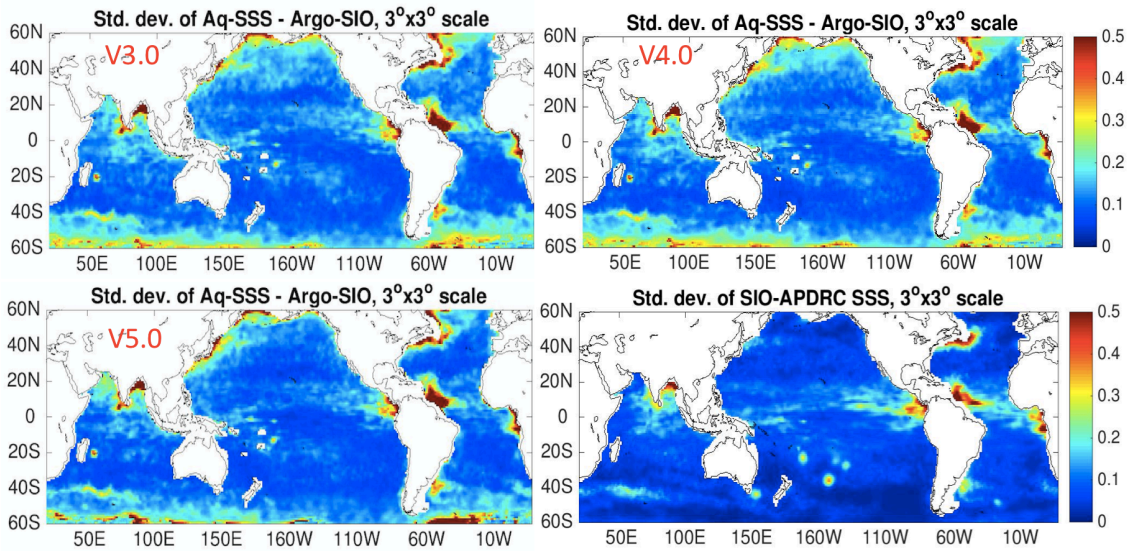

Figure 21. The STD of the difference between Aquarius and Argo-SIO SSS on 3°x3° scale for V3.0, V4.0, and V5.0. The STD of the difference between Argo-SIO and Argo-UH are shown in the lower right panel.

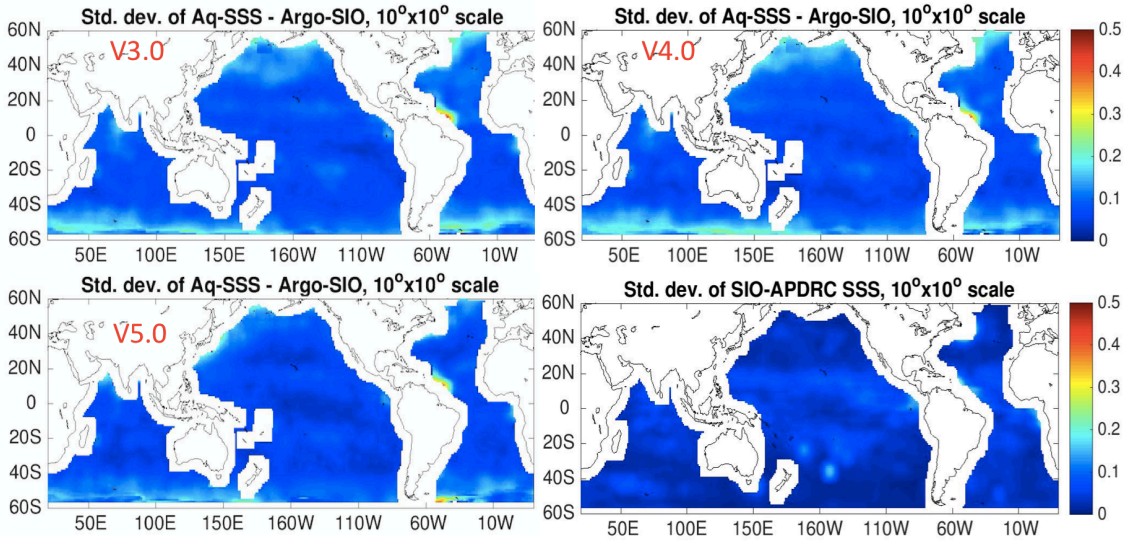

Figure 22. The STD of the difference between Aquarius and Argo-SIO SSS on 10°x10° scale for V3.0, V4.0, and V5.0. The STD of the difference between Argo-SIO and Argo-UH are shown in the lower right panel.

References:

Boutin, J., et al., 2016: Satellite and in situ salinity: understanding near surface stratification and sub-footprint variability. Bull. Amer. Meteorol. Soc., Vol.97, Issue 8, 1391-+, DOI: 10.1175/BAMS-D-15-00032.1. Aug. 2016.

Lee, T. 2016: Consistency of Aquarius sea surface salinity with Argo products on various spatial and temporal scales. Geophys. Res. Lett., 43, 10.1002/2016GL068822.

11. Aquarius Level-3 SSS bias analysis with respect to Argo data (by Oleg Melnichenko and Peter Hacker from University of Hawaii)

Aquarius V5.0 Level-3 SSS data are evaluated against concurrent Argo float measurements. The main focus is on the regional differences and the spurious seasonal signal. To allow a direct comparison with in-situ measurements (variability within a 7-day interval is assumed to be negligible) and with reference to the results from the match-up analysis of Level-2 SSS data, weekly Level-3 SSS maps are used. Argo float measurements shallower than 6 m depth and flagged as good from each Argo profile are used for the analysis (Argo profile data are available at ftp://usgodae.org/pub/outgoing/argo). The difference statistics are computed by comparing Argo float measurements for a given week with SSS values at the same locations obtained by interpolation of the corresponding Level-3 SSS maps. The number of Argo float data per each week in the global ocean is around 1000 with quasi-random geographical distribution (not shown). To provide a comprehensive description of the systematic biases in Aquarius SSS data, the results are presented in three different ways: (1) time-series of the globally averaged bias and root-mean-square difference (RMSD); (2) latitude-time distributions of the zonally averaged bias; and (3) geographical distributions of the time-mean bias and RMSD.

The error statistics for the Level-3 SSS rain-flagged product are presented in **Figure 23**. The time series of the global bias (**Figure 23**) oscillates around zero. The time-mean global bias is smaller than 0.01 psu. There are periods, however, such as in the fall of 2014, when the global bias is significant (e.g., reaching 0.04 psu). The geographical distribution of the time-mean (static) bias is shown in Figure 2b. Large positive biases (up to 0.2 psu locally) are observed in the sub-polar North Pacific and in the Southern Ocean poleward of about 40^{o}S. Large negative biases (up to -0.2 psu) are observed in the subtropical South Pacific and along the continental boundaries. These regions of positive and negative biases tend to cancel each other in the global average, producing nearly zero global bias (**Figure 23a**).

The RMSD between the weekly Level-3 analysis and concurrent Argo float data (**Figure 23c**) is smaller than 0.29 psu for nearly all weeks over the nearly 4-year period of comparison. The mean RMSD over the period September 2011 to May 2015 is 0.247 which is about a 15% improvement compared to version 4.0 (0.29 psu; Melnichenko et al., 2016). The geographical distribution of the RMSD for the weekly Level-3 product is shown in **Figure 23d**. The RMSD are computed in 8^{o}-longitude by 8^{o}-latitude bins to ensure an adequate number of collocations (>100) in each bin. **Over most of the ocean, the RMSD between weekly SSS maps and collocated *in situ* data do not exceed 0.2 psu.** Figure 11-1d also demonstrates that the largest RMSD, exceeding 0.2 psu, are found in the regions of strong variability in SSS, such as along the North Pacific and North Atlantic ITCZ, the North Pacific sub-polar front, the Gulfstream, and near outflows of major rivers such as the Amazon in the tropical North Atlantic. In this regard, the observed relatively large RMSD between the Aquarius and Argo float data in some areas are not necessarily due to errors in Aquarius measurements only, but may include the disparity between time and space scales captured by two different observational platforms (Vinogradova and Ponte, 2012; 2013) and

the difference in measurement depth between Aquarius (ocean surface) and Argo (~5 m depth). The readers are also referred to Section 10 for a related point.

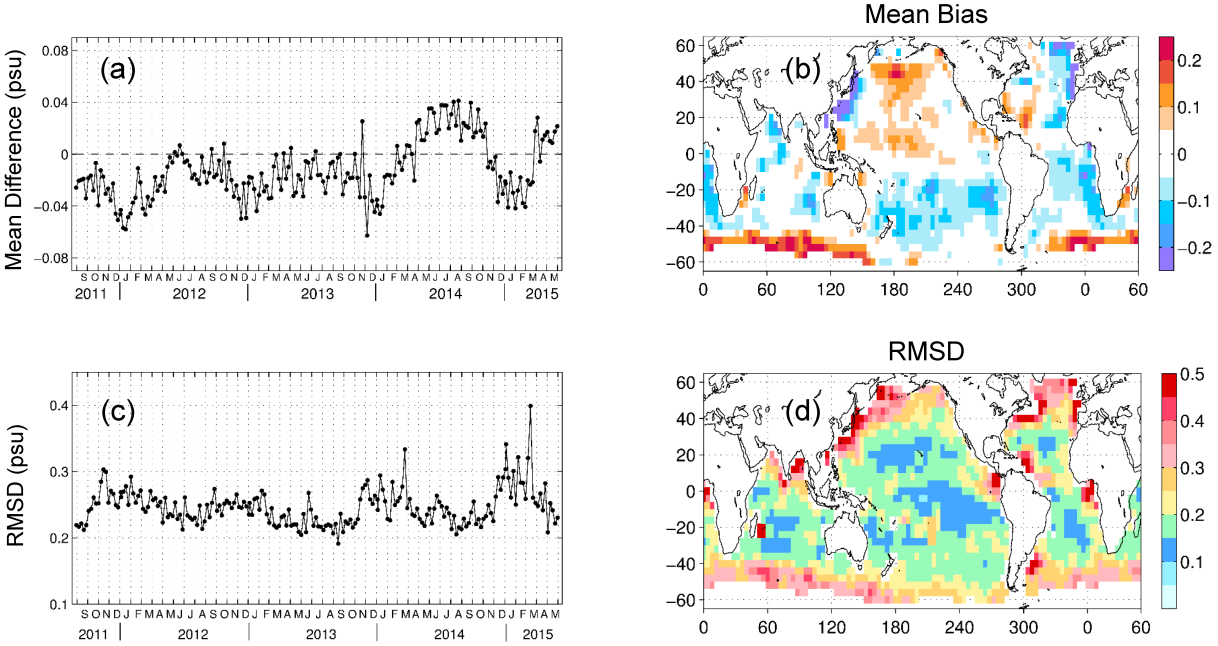

Figure 23. (a) Weekly mean differences (psu), (b) mean spatial bias (psu), (c) weekly RMSD (psu), and (d) geographical distribution of RMSD (psu) between Argo float observations and the Aquarius weekly Level-3 SSS product. The error statistics were computed by comparing Argo float measurements for a given week with SSS values at the same locations obtained by interpolation of the corresponding Level-3 SSS maps. The geographical distributions in (b) and (d) are computed in 8º-longitude by 8º-latitude bins.

To evaluate time variability in the bias fields, **Figure 24** shows the latitude-time distribution of the zonally averaged differences between the weekly SSS maps and the corresponding Argo float data. The zonally averaged biases are calculated weekly by averaging these statistics over 5º-latitude bins. The latitude-time distribution shows significant positive biases at high latitudes and negative biases in the subtropics. Besides the residual static bias, there is a clear seasonal cycle in the bias distribution. To emphasize the time-varying part, the 3-year average (September 2011 to August 2014) in each zonal bin is subtracted from the time series and is shown in **Figure 24b**. The time-varying bias apparently consists of two components: one is a standing oscillation and the other is some kind of a propagating wave, which propagates from the Southern Hemisphere to the Northern Hemisphere with the annual period (shown by the arrow in **Figure 24b**). The peak-to-peak amplitude of the spurious annual cycle can reach 0.2 psu locally. Whether this is significant or not depends on the amplitude of the "true" annual cycle in SSS and the signal-to-noise ratio.

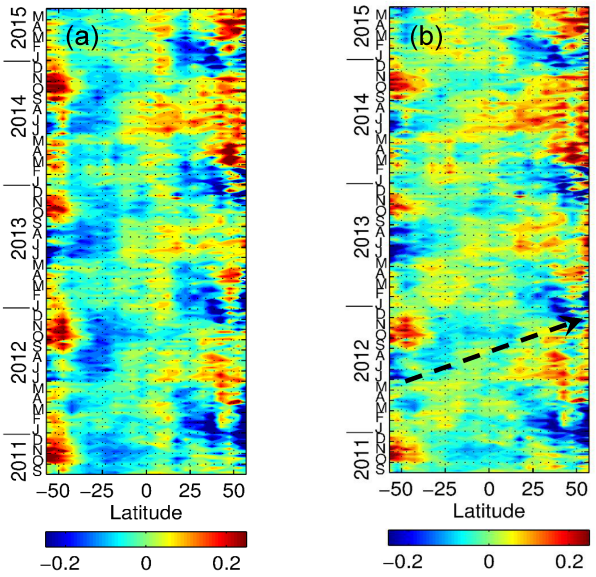

Figure 24. **(a) Latitude-time distribution of the zonally averaged differences (psu) between the weekly Level-3 SSS maps and the corresponding Argo float data. The error statistics were computed by comparing Argo float measurements for a given week with SSS values at the same locations obtained by interpolation of the corresponding Level-3 SSS maps. The zonally averaged biases were computed by averaging these statistics over 5º-latitude bins. (b) The same as in (a), but with the 3-year mean (September 2011 to August 2014) subtracted. The dashed arrow indicates a weak northward propagating signal.**

The geographical distribution of the spurious seasonal signal in Aquarius SSS is assessed against the Argo-derived gridded SSS fields produced by the Asia-Pacific Data Research Center (APDRC) of the University of Hawaii (http://apdrc.soest.hawaii.edu/projects/argo/). Because the Argo-derived product is very smooth, to match the spatial scales, the weekly Level-3 SSS maps from Aquarius were smoothed with a 2D running Hanning window of half-width of 6º, generally consistent with the smoothness properties of the Argo-derived salinity fields. The amplitudes of the spurious annual and semi-annual signals in Aquarius data are determined by the harmonic analysis of the time series of the differences between the gridded Aquarius and Argo data.

The amplitudes of the annual harmonic in the bias fields are presented in **Figure 25a**. Over most of the ocean, the amplitude of the spurious annual signal in Aquarius SSS is smaller than 0.05 psu. There are a few areas, however, where the amplitudes can reach 0.2 psu and more: the western boundary areas in the North Pacific and North Atlantic, the eastern boundary region of the North Atlantic, a zonal band going along the Southern Ocean, the Bay of Bengal and the Arabian Sea in the Indian Ocean, as well as a relatively small area in the eastern equatorial Pacific. Compared to the annual cycle in the Argo gridded SSS data (**Figure 25b**), the difference from the annual signal in Aquarius SSS appears to be minor,

except for the areas described above. The Aquarius data users are therefore advised to exercise caution when analyzing seasonal variability in these areas.

The amplitudes of the semi-annual harmonic in the bias fields are presented in **Figure 25c**. For comparison, the amplitudes of the semi-annual cycle in the Argo-derived SSS fields are presented in **Figure 25d**. Although generally small compared to the spurious annual cycle biases, the semi-annual harmonic in the time-varying bias can be important compared to the Argo-derived variability regionally. Significantly affected areas are in the subtropical South Pacific, particularly along a quasi-zonal band stretching across the basin from about 30°S in the east to close to the equator in the west, and along the Southern Ocean.

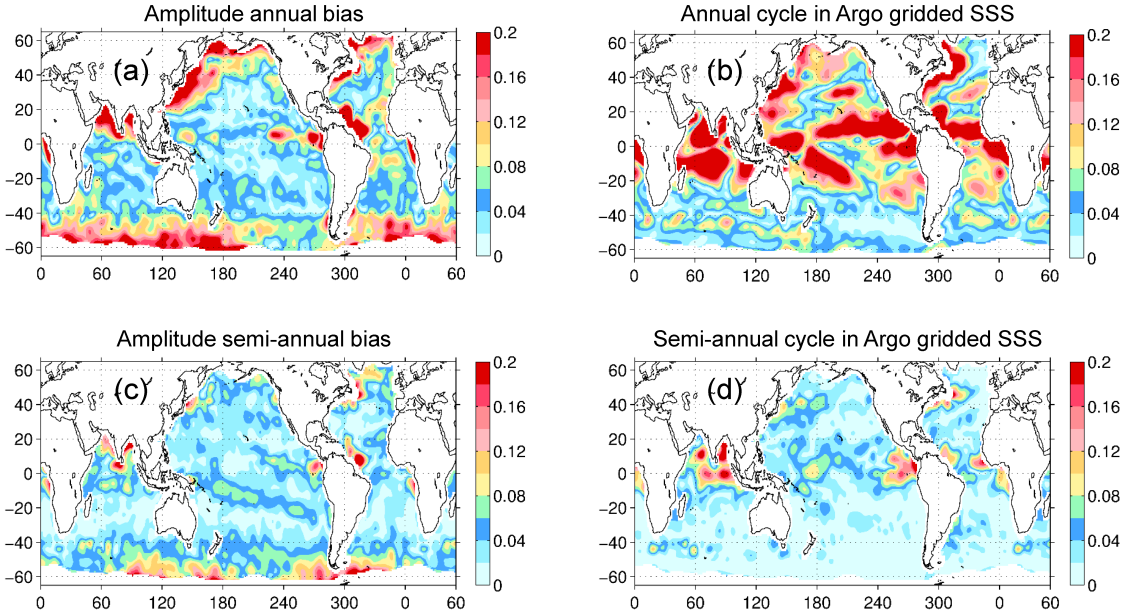

Figure 25. (a) Amplitude of the annual cycle in the Aquarius minus Argo bias. (b) Amplitude of the annual cycle in SSS from the Argo-derived gridded SSS fields produced by the APDRC. (c) Amplitude of the semi-annual cycle in the Aquarius minus Argo bias. (d) Amplitude of the semi-annual cycle in SSS from the Argo-derived gridded SSS fields produced by the APDRC.

Although an attempt has been made to quantify seasonal biases in Aquarius SSS, the results should rather be viewed as semi-quantitative, serving as both a guidance and a note of caution.

References:

Melnichenko O., P. Hacker, N. Maximenko, G. Lagerloef, and J. Potemra (2016), Optimum interpolation analysis of Aquarius sea surface salinity, *J. Geophys. Res.*, 121, 602-616.

Vinogradova, N. T., and R.M. Ponte (2012), Assessing temporal aliasing in satellite-based surface salinity measurements, *J. Atmos. Oceanic Technol.*, 29, 1391-1400.

Vinogradova, N. T., and R.M. Ponte (2013), Small-scale variability in sea surface salinity and implications for satellite-derived measurements, *J. Atmos. Oceanic Technol.*, 30, 2689-2694.

12. Summary, Conclusions and Cautions

This analysis documents the improvements from V2.0 to V5.0 science data processing and their effect on the Aquarius salinity data. By various measures, the RMS errors are reduced in each version.

In this report, Data Version 5.0 has been evaluated with multiple approaches. Regarding the data accuracy on monthly 1x1 degree scales, the results consistently demonstrate that V5.0 errors are less than the mission requirement of 0.2 psu. In Section 4, the triple-point analysis resolved RMSE ~0.17 for point comparisons (no monthly averaging). On monthly time scales, Section 6 triple-point analysis demonstrated a nominal RMSE ~0.128, improving on the mission requirement by a substantial margin. Independent analyses by T.Lee (Section 10) resolved monthly RMSD between gridded Aquarius and Argo data fields to be consistently <0.2. In Section 11, O. Melnichenko and P. Hacker found that over most of the ocean, the RMSD between weekly SSS maps and collocated *in situ* data do not exceed 0.2. ***All of these results present consistent evidence that the Aquarius Ocean Salinity Mission has met and exceeded the measurement accuracy requirement.***

12.1 Important achievement in each version

V2.0: The V2.0 data is separating the sensor calibration variations from time-varying errors in the geophysical corrections. This has removed the quasi-monthly, non-monotonic variations seen in the V1.3 data. The scatterometer VV-pol cross section has been included in the surface roughness correction. In addition to the NCEP wind speed, which reduces the retrieval error from V1.3.

V3.0: The V3.0 surface roughness correction uses Aquarius wind speeds and scatterometer VV-pol cross section instead of NCEP wind speeds. The Aquarius wind speeds are based on scatterometer HH-pol and radiometer H-pol measurements. Both V-pol and H-pol radiometer channels are used in the maximum likelihood estimator (MLE) of the salinity retrievals. This new roughness correction and the inclusion of the H-pol in the MLE further reduce the retrieval error of the L2 product. The V3.0 data has also a better correction for the reflected galaxy, which uses an empirical symmetrization between the ascending and the descending swaths. This has greatly reduced the amplitude and the seasonal variations of the ascending and descending differences, particularly in the Southern Ocean. V3.0 shows noticeable positive biases in the high latitude, and negative biases in the low latitudes. An empirical post-hoc SST bias correction was

implemented, which is applied to the retrieved salinity. This post-hoc correction mitigates the observed zonal biases. Quality control flags have been included in the L2 product.

V4.0: The empirical post-hoc SST bias correction has been refined and integrated into the geophysical model function that is used in the retrievals. This resulted in a further reduction of the observed regional biases and a further reduction in the retrieval error. Formal uncertainty estimates for the retrieved salinity have been included.

V5.0: The model of the atmospheric oxygen absorption and the SST dependence of the surface correction have been changed. The empirical post-hoc SST bias correction from V3.0 and V4.0 have been eliminated. The reflected galaxy correction has been improved based on SMAP observations. This resulted in a significant reduction of the remaining zonal and temporal biases that were still present in V4.0, in particular in the N Pacific and at high S latitudes. V5.0, the rain masks are applied to remove the biases that are caused by the strong precipitation. The reference SST input data are changed to the CMC SST product from NCEI, in place of the NOAA SST used in prior versions (see [3]).

12.2 Notes of Caution

Localized persistent biases between ascending and descending passes could be linked to radio frequency interference (RFI) that is not completely corrected by the RFI filter. The RFI will bias the brightness temperatures toward the positive, thus the salinity will be biased negative. These regions are primarily in the eastern N. Atlantic adjacent to Europe where it is likely that the ascending pass is contaminated as the antenna faces the European subcontinent. Likewise, the western N. Atlantic and Asia-Pacific regions are biased on the descending pass when the antenna views westward. From V3.0, Flag #23 (See table 1 in Aquarius_Level-2_Data_Products_5.0.pdf) is added to exclude the area with unacceptable asc/dsc differences. This flag identifies areas where the asc/dsc difference is sufficiently large that the data from the out-of-bound pass (i.e. either asc or dsc) is discarded for purposes of calibration. The algorithm is to be provided by T. Meissner [See AQ-014-PS-0006_ ProposalForFlags&Masks_DatasetVersion3.0, which is included in the Data Version V5.0 documentation.]. **Figure 5** shows that the eastern N. Atlantic and the eastern N. Indian

Ocean are masked out in the ascending map, and the western N. Atlantic and Pacific are masked out in the descending map.

Note of Caution, RFI: Persistent negative salinity bias may be present in some regions due to RFI. Users should be very cautious with using ascending pass data in the eastern N. Atlantic and descending pass data in the western N. Atlantic and Asia-Pacific regions.

Note of Caution, rain masks: The rain masks are added in V5.0 for both L2 and L3 data. If the users are interested in the Aquarius SSS under strong precipitation, the data without rain masks should be used. Otherwise, data with rain masks should be used for general studies. The users can tell if the data has been rain masked from the file titles.

Note of Caution, land fraction in the Level 3 mapped data: The ADPS data uses land fraction of 0.01 (severe) for the criterion to include more data information near the coast. However, regions with land fraction between 0.01 and 0.001 are included in the mapped data with larger biases due to the land contaminations. The users should be aware the biases in these regions as discussed in Section 6 & 9.

Note of Caution, regionally dependent static and time-varying biases: Users should be aware of Aquarius SSS biases with respect to in situ data such as Argo in regions where such biases are not expected, especially with regard to annual and semi-annual variability. Mostly such biases are small, but in some regions the bias amplitudes are larger than the signals observed by in situ data as discussed in Section 5, 8 and 11.

13 References

1. Lagerloef, G., R. Colomb, D. Le Vine, F. Wentz, S. Yueh, C. Ruf, J. Lilly, J. Gunn, Y. Chao, A. de Charon , G. Feldman, and C. Swift; The Aquarius/SAC-D mission –Designed to Meet the Salinity Remote Sensing Challenge, Oceanography, Volume 21(1), 68-81, 2008.
2. Le Vine, D.M., G.S.E. Lagerloef, F.R. Colomb, S.H. Yueh, and F.A. Pellerano. 2007. Aquarius: An instrument to monitor sea surface salinity from Space IEEE Transactions on Geoscience and Remote Sensing 45 (7): 2,040–2,050.
3. Meissner, T., F. Wentz and D. Le Vine, 2017: Aquarius V5.0 Algorithm Theoretical Basis Document (ATBD). See [10].
4. Aquarius Radiometer Post-Launch Calibration for Product Version 2. See [10].
5. Reynolds, R. W., T. M. Smith, C. Liu, D. B. Chelton, K. S. Casey, and M. G. Schlax, 2007: Daily high-resolution blended analyses for sea surface temperature. J. Climate, 20, 5473-5496.
6. Brasnett B., 2008: The impact of satellite retrievals in a global sea-surface-temperature analysis. Q.J.R. Meteorol. Soc., 134, 1745-1760. DOI: 10.1002/qj.319
7. Chassignet, E.P., H.E. Hurlburt, E.J. Metzger, O.M. Smedstad, J. Cummings, G.R. Halliwell, R. Bleck, R. Baraille, A.J. Wallcraft, C. Lozano, H.L. Tolman, A. Srinivasan, S. Hankin, P. Cornillon, R. Weisberg, A. Barth, R. He, F. Werner, and J. Wilkin, 2009. U.S. GODAE: Global Ocean Prediction with the HYbrid Coordinate Ocean Model (HYCOM). Oceanography, 22(2), 64-75.
8. E.J. Metzger, O.M. Smedstad, P. Thoppil, H.E. Hurlburt, A.J. Wallcraft, D.S. Franklin, J.F. Shriver, and L.F. Smedstad, 2008: Validation Test Report for the Global Ocean Prediction System V3.0 – 1/12° HYCOM/NCODA: Phase I. NRL Memo. Report, NRL/MR/7320--08-9148.
9. E.J. Metzger, O.M. Smedstad, P.G. Thoppil, H.E. Hurlburt, D.S. Franklin, G. Peggion, J.F. Shriver, T.L. Townsend, and A.J. Wallcraft, 2008: Validation Test Report for the Global Ocean Prediction System V3.0 – 1/12° HYCOM/NCODA: Phase II. NRL/MR/7320--10-9236.
10. Aquarius data technical documents are located on the PO.DAAC Aquarius page.

Appendix A: The NAVO/FSU HYCOM data are obtained from the global 1/12° data-assimilative HYCOM model along with the Navy Coupled Ocean Data Assimilation (NCODA) system at the Naval Oceanographic Office (NAVOCEANO). The HYCOM data are available from the HYCOPM data server http://tds.hycom.org/thredds/GLBa0.08/expt_90.9.html?dataset=GLBa0.08/expt_90.9.

This HYCOM run assimilates available along track satellite altimeter observations, satellite and in situ sea surface temperature as well as in situ vertical temperature and salinity profiles from XBTs, ARGO floats, and moored buoys. In terms of near surface salinity forcing, HYCOM uses monthly climatology of river discharges (applied at the top 6 meters of the model) and relaxation to monthly SSS climatology (at 15 m) with a restoring time scale of 30 days, in addition to E-P forcing. Both the climatological river forcing and near surface salinity relaxation are intended to prevent the HYCOM simulation from drifting away from climatology, but at the same time they may suppress non-seasonal variations occurring in nature. The NCODA system is based on a multi-variate Optimal Interpolation (MVOI) scheme. Because of the assimilation of Argo floats and buoy data, the HYCOM analysis is not independent of Argo and buoys. Moreover, the nature of the assimilation could also introduce some level of correlation between the errors of the HYCOM analysis field and the errors of Argo and buoy SSS. More details of this HYCOM solution can be found in [7], [8] and [9].

Appendix B: Triple point uncertainty estimate of Aquarius and validation data

The satellite salinity measurement S_S and the *in situ* validation measurement S_V are defined by:

$$S_S = S \pm \varepsilon_S$$

$$S_V = S \pm \varepsilon_V$$

where S is the true surface salinity averaged over the Aquarius footprint area and microwave optical depth in sea water (~ 1 cm). ε_S and ε_V are the respective satellite and *in situ* measurement errors relative to S. The mean square of the difference ΔS between S_S and S_V is given by:

$$\langle \Delta S_{SV}^2 \rangle = \langle \varepsilon_S^2 \rangle + \langle \varepsilon_V^2 \rangle \quad (1)$$

where $\langle\ \rangle$ denotes the average over a given set of paired satellite and *in situ* measurements, and $\langle \varepsilon_S \varepsilon_V \rangle = 0$.

Likewise, define HyCOM salinity interpolated to the satellite footprint as $S_H = S \pm \varepsilon_H$, and mean square differences

$$\langle \Delta S_{HV}^2 \rangle = \langle \varepsilon_H^2 \rangle + \langle \varepsilon_V^2 \rangle \quad (2)$$ HyCOM vs in situ validation data

$$\langle \Delta S_{SH}^2 \rangle = \langle \varepsilon_S^2 \rangle + \langle \varepsilon_H^2 \rangle \quad (3)$$ Satellite vs HyCOM

Equations (1)-(3) comprise three equations with three variables given by:

$$\langle \varepsilon_S^2 \rangle = \{\langle \Delta S_{SV}^2 \rangle + \langle \Delta S_{SH}^2 \rangle - \langle \Delta S_{HV}^2 \rangle\}/2 \quad (4)$$ satellite measurement error

$$\langle \varepsilon_H^2 \rangle = \{\langle \Delta S_{SH}^2 \rangle + \langle \Delta S_{HV}^2 \rangle - \langle \Delta S_{SV}^2 \rangle\}/2 \quad (5)$$ HyCOM measurement error

$$\langle \varepsilon_V^2 \rangle = \{\langle \Delta S_{SV}^2 \rangle + \langle \Delta S_{HV}^2 \rangle - \langle \Delta S_{SH}^2 \rangle\}/2 \quad (6)$$ In situ validation measurement error

End of document